Progress in Oceanography 208 (2022) 102903

Contents lists available at ScienceDirect

Progress in Oceanography

journal homepage: www.elsevier.com/locate/pocean

East Siberian Sea: Interannual heterogeneity of the suspended particulate matter and its biogeochemical signature

Oleg Dudarev [a,d,*], Alexander Charkin [a], Natalia Shakhova [a,b,c,d], Aleksey Ruban [e], Denis Chernykh [a,d], Jorien Vonk [f], Tommaso Tesi [g], Jannik Martens [h], Irina Pipko [a], Svetlana Pugach [a], Elena Gershelis [d,e], Andrey Leusov [a], Andrey Grinko [e], Örjan Gustafsson [i], Igor Semiletov [a,d,j]

[a] V.I. Il'ichev Pacific Oceanological Institute (POI), Russian Academy of Sciences, Far Eastern Branch, Vladivostok, Russia
[b] Department of Chemistry, Moscow State University, Moscow, Russia
[c] International Arctic Research Center (IARC), University of Alaska Fairbanks, Fairbanks, USA
[d] Tomsk State University, Tomsk, Russia
[e] Tomsk Polytechnic University, Tomsk, Russia
[f] Vrije Universiteit Amsterdam, Department of Earth Sciences, Faculty of Science, The Netherlands
[g] Institute of Polar Sciences (ISP-CNR), Bologna, Italy
[h] Lamont-Doherty Earth Observatory, Columbia University, NY, USA
[i] Department of Environmental Science and the Bolin Centre for Climate Research, Stockholm University, Sweden
[j] Institute of Ecology, Higher School of Economics (HSE), Moscow, Russia

A R T I C L E I N F O

Keywords:
Arctic
East Siberian Sea
Suspended particulate matter transport
Organic matter
Spatial and interannual variability

A B S T R A C T

The East Siberian Sea (ESS) is the largest, shallowest and most icebound Arctic marginal sea. It receives substantial input of terrigenous material and climate-vulnerable old organic carbon from both coastal erosion and rivers draining the extensive permafrost-covered watersheds. This study focuses on the interannual variability and spatial distribution of suspended particulate matter (SPM) in the surface and bottom waters of the ESS during the ice-free period in 2000, 2003, 2004, 2005 and 2008. We report on the composition and variability of particulate organic carbon (POC), total nitrogen (TN), POC/TN ratios, carbon and nitrogen isotopes ($\delta^{13}C$, $\delta^{15}N$) and provide estimates of the contribution of terrestrial organic carbon (terrOC) based on the $\delta^{13}C$ isotopic values.

The results show that interannual SPM distribution and elemental-isotopic characteristics of POC differ significantly between the western biogeochemical province (WBP; West of 165°E) and the eastern biogeochemical province (EBP; East of 165°E) of the ESS. The SPM mean concentration in the WBP is almost an order of magnitude higher than in the EBP. From west-to-east of the ESS, SPM tends to become more depleted in $\delta^{15}N$, while the $\delta^{13}C$ becomes isotopically heavier. This trend can be explained by a shift in organic matter sources from terrigenous origin (erosion of the coastal ice complex and riverine POC) to becoming dominantly from marine plankton.

The maximum contribution of terrOC to POC reached 99% in parts of the WBP, but accounts for as low as 1% in parts of the EBP. At the same time, the type of atmospheric circulation and its associated regime of both water circulation and ice transport control a displacement of the semi-stable biogeochemical border between WBP and EBP to the east or to the west if compared to its long-term average position near 165°E. Our multi-year investigation provides a robust observational basis for better understanding of the transport and fate of terrigenous material upon entering the ESS shelf waters. Our results also provide deeper insights into the interaction in the land-shelf sea system of the largest shelf sea system of the World Ocean, the East Siberian Arctic Shelf system.

* Corresponding author.
E-mail address: dudarev@poi.dvo.ru (O. Dudarev).

https://doi.org/10.1016/j.pocean.2022.102903
Received 18 November 2021; Received in revised form 13 September 2022; Accepted 21 September 2022
Available online 27 September 2022

1. Introduction

The Arctic Region is warming at a much higher rate than other parts of the planet affecting the global and regional carbon cycles. Global climatic changes are expected to induce remobilization of vulnerable "old" carbon currently freeze-locked in the permafrost deposits. As permafrost soils store substantial amounts of carbon (~1300 Pg; Hugelius et al., 2014), the scale of this remobilization and its potential effect on Arctic marine ecosystems and global climate are still a matter of ongoing debate (e.g., Minsley et al., 2012; Vonk and Gustafsson, 2013; Schuur et al., 2015; Biskaborn et al., 2019; Turetsky et al., 2020). It is therefore important to better constrain the mechanisms and pathways of permafrost carbon transport and transformation in the Arctic Ocean.

The East Siberian Arctic Shelf (ESAS), which includes the Laptev Sea, the East Siberian Sea (ESS), and the Russian part of the Chukchi Sea, is the world's largest continental shelf. Great Russian Arctic Rivers supply a vast amount of terrestrial organic carbon (terrOC) into the shelf waters (Guo et al., 2004; Stein and Macdonald, 2004; van Dongen et al., 2008; Gustafsson et al., 2011; Tesi et al., 2014; Wild et al., 2019). In addition, an important part of the terrOC delivered to the ESAS is transported in particulate form (particulate organic carbon, POC) associated with suspended particulate matter (SPM). The SPM is derived from several sources, including importantly from the continuous erosion of the coastlines but also from catchments and from marine plankton (e.g, Vonk et al., 2012).

The ESS is ice-covered on average 10 months per year and despite its size remains one of the least explored high-latitude seas. Distribution and transformation of the SPM as well as associated POC in the ESS occur in a vast mixing zone of fresh and salt waters in a short ice-free period. Due to limited access to the ESS for field studies, there is still lack of understanding how terrOC behaves upon entering the ESS waters. Most studies performed in the ESS have focused on sedimentary organic carbon (OC) sources and degradation status (e.g., Bröder et al., 2016; Feng et al., 2013, 2015a,b, Martens et al., 2020, 2021; Salvadó et al., 2015; Semiletov et al., 2005; Tesi et al., 2014, 2016, Vonk et al., 2010, 2012, 2014), while studies on the POC sources and transport pathways have presented temporally and spatially limited results. First data about sources and fate of terrestrial POC in the Arctic Seas appeared in the first decade of our century (Stein and Macdonald, 2004; Semiletov et al., 2005; Guo et al., 2007). Later important insights into the sources and transformation of terrestrial POC while being transported across the ESAS were gained with complex molecular- and isotopic-based studies (e.g., Charkin et al., 2011; Doğrul Selver et al., 2015; Karlsson et al., 2016; McClelland et al., 2016; Salvadó et al., 2016; Sánchez-García et al., 2011; Vonk et al., 2010; Karlsson et al., 2011). At the same time, interannual variability of SPM and POC characteristics has remained insufficiently investigated, even for the ice-free periods.

In this study we present the results of a multi-year interdisciplinary study based on a series of unique field observations in the ESS land-shelf system in 2000, 2003, 2004, 2005 and 2008, performed by an international team of researchers. Here we aim to identify trends of spatial and interannual variability of SPM and its POC in the poorly explored ESS by presenting the first detailed overview of the distribution, transport and biogeochemistry of the SPM across the ESS. These data provide a robust observational basis towards a better understanding of SPM and associated terrestrial POC behaviour in the Pan-Arctic land-shelf system under ongoing climate change.

2. Study area

The ESS is one of the broadest and shallowest shelf seas in the World Ocean, extending over 1200 km from the adjacent Laptev Sea in the west to the Chukchi Sea in the east. The ESS covers an area of ~ 890 000 km^2 with a mean depth of 58 m. Given its large extent and shallow depths, the volume of sea water is only 61 000 km^3, which is 6 times lower if compared to the Laptev Sea. The ESS is one of the coldest high-latitude seas (Geoecology of shelf and coasts of Russian Seas, 2001; Navigation Book of the East-Siberian Sea, 1998). The area covered by this study is almost the entire shallow ESS, from the coastline to the shelf edge and the upper slope of the Arctic Basin (Fig. 1).

The hydrological water balance of the ESS is dominated by melt water (77 %) and only 17 % comes from river runoff. The average annual freshwater input is estimated at 1240 km^3 with its interannual variability about 24 % (Nikiforov and Shpayher, 1980). The large freshwater supply results in a decrease in the ESS surface water salinity by 10–15 ‰. For comparison, the waters of the Central Arctic Basin north of the ESS have about ~ 32–34 ‰ (Anderson et al., 2013). This indicates that the greatest part of the ESS is a mixing area (at least in the ice-free period), where the boundary for the ambient Arctic Seas is a characteristic isohaline of 25 ‰ (Nikiforov and Shpayher, 1980; Osadchiev et al., 2021).

The total terrigenous sediment export from the ESS drainage basin accounts for ~ 122 Mt/yr. The main sources of sediments supply are (i) coastal erosion of the Late Pleistocene Ice Complex Deposits (ICD) (67.6 Mt/yr, 55.4 %), (ii) SPM exported from both Indigirka and Kolyma, the largest rivers discharging into the ESS (21.9 Mt/yr, 18 %), and (iii) coastal erosion of other coastal types (non-ICD) (20.0 Mt/yr, 16.4 %). Sea ice transport (ice cryosol) and aeolian transport, accounting together for 10.2 % of the total sediment export, translocate 12.1 Mt/yr and 0.4 Mt/yr, respectively.

Within the ESS, the total OC content present as SPM is estimated to be 16.4 Mt, of which most is produced locally as primary production from phytoplankton (7.0 Mt C/yr, 42.3 %) followed by cryophilic phytoplankton production (4.7 Mt C/yr, 28.3 %). Additionally, ESS SPM is estimated to hold terrigenous OC from ICD erosion ("old" remobilized carbon; 2.4 Mt C/yr, 14.5 %), river SPM (biomass of freshwater plankton, remnants of terrestrial vegetation and OC sorbed by high-molecular colloids and iron hydroxides on clay particles; 1.9 Mt C/yr, 11.2 %). A minor fraction is thought to consist of ice cryosol and aeolian transport, together contributing about 0.4 Mt C/yr (2.6 %) (Rachold et al., 2003; Gordeev et al., 1996; Gordeev and Rachold, 2004; Grigoryev et al., 2004; Vetrov and Romankevich, 2004; Shevchenko and Lisitzin, 2004; Dudarev et al., 2016).

The ESS is characterized by an extremely large gradient of hydrological and biogeochemical parameters extending from Long Strait in the east (south of Wrangel Island) to the Dmitry Laptev Strait in the west (south of the New Siberian Islands). The ESS is also divided into two different biogeophysical regimes with sharp geographical contrasts in hydrological and biogeochemical properties where the pacific water to the east meets in a frontal zone the local river-influenced shelf waters from the west (Nikiforov and Shpaikher, 1980; Semiletov et al., 2000, 2005). A major plume of riverine freshwater usually transits the ESS eastward along the coastal zone termed the Siberian Coastal Current (SCC). Based on the hydrological and hydrochemical data, one can identify-two provinces: the western biogeochemical province (WBP) is strongly influenced by the Lena River transporting both heat and freshwater flux, and by the SPM transport induced by coastal erosion, while the eastern biogeochemical province (EBP) is characterized by pacific-derived waters. From year to year, the longitude shift of the frontal zone, bounded by isohaline 25 ‰, between WBP and EBP may reach 10° and more (Semiletov et al., 2005; Pipko et al., 2011). Temperature, salinity and hydrochemical data show that winds mixed the water column from the top to the bottom in the WBP (roughly between 140° E and 160° E). The WBP is characterized by low primary productivity and high concentration of terrigenous SPM containing large fraction of old terrOC released by coastal erosion. Degradation of the remobilized terrOC causes a decrease in both pH values and dissolved oxygen concentrations (Semiletov et al., 2016), while the partial pressure of carbon dioxide and its acidification impact are increased (Anderson et al., 2011; Pipko et al., 2011; Semiletov et al., 2016). If compared to WBP, contribution of SPM and associated POC in the EBP is

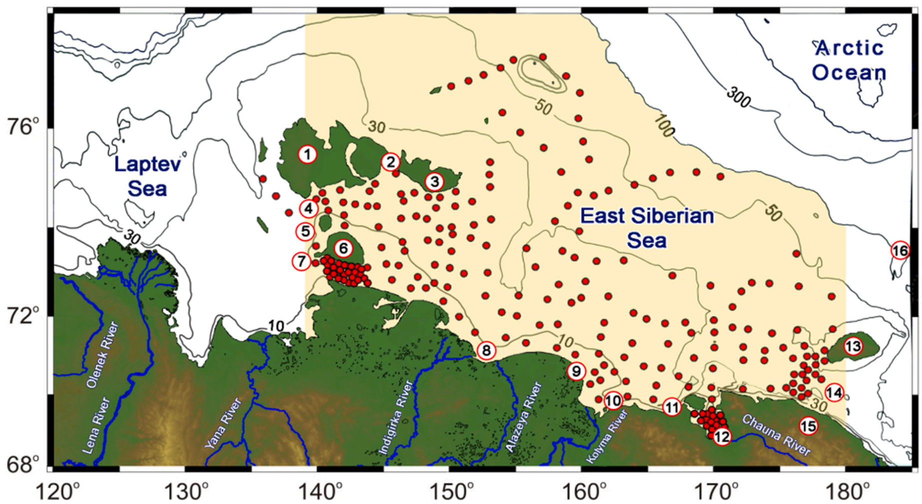

Fig. 1. The ESS (borders are marked by yellow shading) sampling stations (red dots) at September 2000, 2003, 2004, 2005 and 2008. Number in circles identify geographical areas mentioned in the text: 1 – Kotelny Island (New Siberian Islands), 2 - Blagoveszhensky Strait, 3 - Novaya Sibir Island (New Siberian Islands), 4 - Sannikov Strait, 5 - Maliy Lyakhovsky Island and 6 - Bolshoy Lyakhovsky Island (Lyakhovsky Islands)., 7 - Dmitry Laptev Strait, 8 - Indigirka Gulf, 9 – Chukochy Cape, 10 - Kolyma Gulf, 11 - Ayon Island, 12 – Chaun Gulf, 13 - Wrangel Island, 14 - Long Strait, 15 - Chukchi Peninsula, 16 - Herald Canyon.

much lower; the saltier and colder EBP located eastwards of ~ 160°-170° E is mainly affected by nutrient-rich pacific waters creating favourable conditions for high summer primary production. General characteristics of the ESS and its catchment basins are given in the Supplementary Text S1.

Global warming resulting in shifting atmospheric moisture patterns along with arctic permafrost degradation may accelerate river discharge (Savelieva et al., 2000) and carbon remobilization from soils. The role of the ESS in transport and fate of freshwater and terrOC has not been sufficiently discussed.

3. Materials and methods

3.1. Sampling

The observational part of this study is based on measurements performed at 312 oceanographic stations varying between 2.5 m and 100 m depth and covering an area from the upper part of the underwater coastal slope to the shelf edge (Fig. 1). CTD sounding and sampling was done onboard the hydrographic vessels “Nikolay Kolomeytsev”, “Ivan Kireev”, “Yakov Smirnitskiy” and the special vessel “Auga” in the ice-free period of 2000, 2003, 2004, 2005 and 2008 (Table 1).

Table 1
A list of expeditions reaching the East Siberian Sea (ESS), CTD measurement types and sensors.

Research vessels	Dates in the ESS	CTD type	Sensors
“Nikolay Kolomeytsev”	2000, September 06–12	Memory STD (ALEC Electronics)	pressure, temperature, conductivity
“Ivan Kireev”	2003, September 13–21	SeaBird Seacat 19+	pressure, temperature, conductivity
“Ivan Kireev”	2004, September 01–14	SeaBird Seacat 19+	pressure, temperature, conductivity
“Auga”	2005, September 14–23	SeaBird Seacat 19+	pressure, temperature, conductivity
“Yakov Smirnitskyi”	2008, September 01–15	Seabird SBE 9	pressure, temperature, conductivity, turbidity (Wetlabs)

Studies were carried out during the eastern (ET regime) anticyclonic type (2000, 2005, 2008) and western (WT regime) cyclonic type (2003, 2004) resulting in specific water circulation patterns. The ET is characterized by a prevalence of air mass transport from the east to the west and advection to the EBP of the pacific waters and thus weakening of the Siberian Coastal Current (SCC). In contrast, WT is characterized by a prevalence of air masses transferring from the west to the east, which diminishes the water flux from the Chukchi Sea to the EBP and increases the SCC (Proshutinsky and Johnson, 1997; Savelieva et al., 2000; Semiletov et al., 2000; Proshutinsky et al., 2012). Table 2 shows an increase in the input of East Siberian Rivers by 2008, as well as a decrease in the ice-covered area in the Arctic Basin. Such trends are expected to affect the interannual variability of the SPM characteristics, and this is further confirmed by the extensive field observational data of the present study (see below).

3.2. Analytical methods

Surface (upper 0.5 m) and near bottom (1 m from bottom) water was filtered using a PVC filter holder from ThermoScientific. Samples were taken with a 25 L Niskin bottle. For determination of the SPM weight content using the «Advantec» filters 0.45 μm (an analytical balance “Adventurer Ohaus”, measurement accuracy is 0.0001 g).

SPM also collected by pumping water through a glass fiber filter (GF/F) 0.7 μm. Filters is pre-combusted (6 h, 450 °C) and were after filtration immediately transferred to pre-combusted aluminium envelopes, frozen and kept at − 18 °C until analysis.

Table 2
Interannual river runoff and hydrometeorological conditions during 2000, 2003, 2004, 2005 and 2008.

River runoff (km^3/yr) and hydrometeorological regime	2000	2003	2004	2005	2008	Average for 1936–2000
Lena River[a]	616	443	558	596	705	535
Yana River[a]	27	32	32	46	50	32
Kolyma River[a]	89.5	85.4	120	86.2	113.7	102.6*
Indigirka River[a]	no data	no data	no data	no data	no data	50.1
Type of atmospheric macroprocesses and hydrological regime	ET	WT	WT	ET	ET	–
Ice-free sea area, % [b]	35	60	45	70	90	–

[a] https://rims.unh.edu;
[b] https://www.aari.ru

The POC and its $\delta^{13}C$, TN and $\delta^{15}N$ contents were measured either at the International Arctic Centre (Alaska State University, Fairbanks, USA) or at Stockholm University (Department of Environmental Science) with a Carlo Erba NC2500 elemental analyzer, connected via a splite interface to a mass-spectrometer Finnigan MAT Delta Plus. The accuracy and reproducibility of the results of the determination of $\delta^{13}C$ and $\delta^{15}N$ was ± 0.1 ‰ and ± 0.2 ‰, respectively (Guo et al., 2004; Guo and Santschi, 1996; Gustafsson et al., 1997, 2001, Sánchez-García et al.,

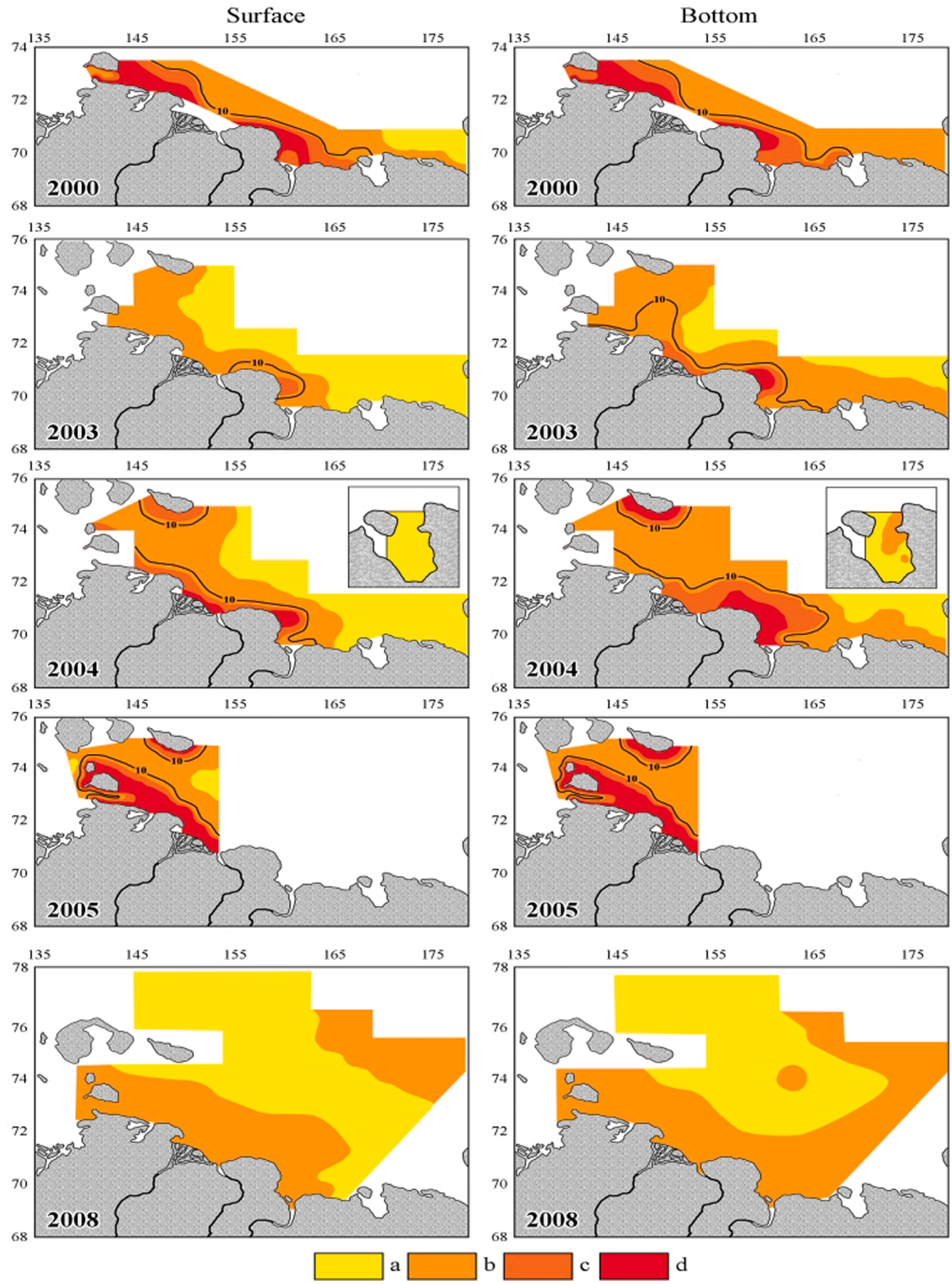

Fig. 2. SPM content during 2000, 2003, 2004, 2005 and 2008. SPM (mg/L): a - < 2, b – 2–13, c – 13–24, d - > 24.

2011, 2014, Vonk et al., 2010, 2012; Karlsson et al., 2011, 2015, 2016).

4. Results and discussion

4.1. Interannual variability of the SPM content

September 2000. The ESS was influenced by the ET regime. The Lena River water discharge exceeded the annual average by 15 %, slightly affecting the freshening of the water. With predominantly northern and northeastern wind direction, the edge of the drifting sea ice was close to the Siberian coast; the same situation was observed for the the subsequent years (Table 2; see Suppplementary Figures, Fig. S1). Sea ice extent in 2000 reached its maximum for the period 2000–2008. The nearshore position of the cold front, together with wind and convective mixing, led to a cooling of the ice-free ESS. Temperature (T) values varied between 1.4 and 4.7 °C for the WBP surface waters and between ~ 0.7–3.6 °C for the WBP bottom waters, while in the EBP those variations were between − 0.9 and 1.4 °C near the surface and between ~ -1.8–0.8 °C at the bottom. The pacific water inflow led to a westward shift of the 0° isoterm (Fig. 2S). Salinity (S) in the WBP varied between 10.4 and 22.3 ‰ in the surface waters and 19.0–25.6 ‰ in the bottom waters, and in the EBP waters it ranged from 27.5 to 31.7 ‰ near the surface and from 31.4 to 33.3 ‰ at the bottom. The influence of the pacific waters resulted in a westward shift of the isohaline 25 ‰ if compared to its average longterm position (Fig. S3). In the WBP, waves increased up to 3 m during the study period, which was followed by a weakening of the wind forcing. By contrast, waves were not higher than 1.5 m in the EBP. Hence, wave mixing affected the entire water column in the WBP, while the water column was only moderately stratified in the EBP.

SPM content in the WBP varied from 4.7 to 79.7 mg/L (mean and median absolute deviation are shown in Table 2) in the surface waters and from 10.6 to 106.4 mg/L near the bottom. This shows that there was no strong water mixing throughout the entire water column, as we observed differences in the SPM concentrations between the surface and bottom waters (Fig. 2). Water of the Indigirka River did not affect the TS-characteristics in the Indigirka Gulf. This might be explained by reduced water discharge in 2000, the same as for the Kolyma River. SPM content in the Indigirka Gulf varied between 39 and 48 mg/L. Off the Indigirka Delta, these elevated SPM concentrations stem from storm-induced resuspension zones that are largely sourcing SPM from ICD erosion. During the summer season, erosion of ICD accelerates in the lower course of the river. The annual coastal retreat ranges from 7 to 28 m/y (cf. Aibulatov, 2001). Therefore, the SPM content in delta waters can reach up to 1000 mg/L , which is comparable to the SPM concentrations in the estuaries of Asian megarivers, such as Yangtze, Huang-He and Mekong (Anikiev et al., 2004; Sternberg et al., 1985; Cao et al., 1986; Zhang and Huang, 1990; DeMaster et al., 2017).

In 2000, the water discharge of the Kolyma River, the largest catchment of the ESS, was below the average. In the Kolyma Gulf surface waters (S < 20 ‰), the SPM content varied between 16 and 47 mg/L with a maximum value observed close to Chukochy Cape, which is known to have the highest rate of coastal erosion (Grigoryev et al., 2004). The river water plume was pressed towards the deeper basin and could be tracked in the Kolyma River Paleovalley (see position of Kolyma Paleovalley at Fig. 3b, transect XI). There seemed to be a hydrological frontal zone in the outer part of the Kolyma Gulf, likely caused by the interaction of the SCC and advection of the pacific waters. This section of the Kolyma Gulf is confined by the boundary between the WBP and the EBP. The water column of the eastern Kolyma Gulf is characterized by lower T (±1 °C) and S (>25 ‰). SPM concentrations ranged between 1.2 and 3.6 mg/L in the surface waters and between − 2.4–7.9 mg/L near the bottom. The location of the isotherm 0 °C near the shore was not observed at this time or subsequent years due to a vast field of drifting pack ice. Near Ayon Island the pack ice approached the shore by 25–40 km. The ice field served as a mechanical obstacle for the SPM transport acting as a natural sedimentation barrier. The SPM content reduced to one fourth on average (Table 3; Figs. 2, S2, S3). SPM was also taken up by freezing water and incorporated into freshly formed ice, which occured along the edges of the perennial ice masses. At the same time, migration of SPM was observed beneath the ice cover. This appears in polynyas when fresh and warmer runoff waters (with a higher SPM content) enter cold salty shelf waters (with a lower SPM content) (cf. Aibulatov, 2001).

September 2003. The ESS region was this year dominated by the WT regime. There was a low-pressure gradient producing weak southerly winds and almost no wind on the sea surface with a residual swell of only 1 m. Since the beginning of the 21st century, the ice-free area of the ESS has increased annually. It occupied only 20 % in 1999 increasing up to 35 % in 2000 and reaching 60 % in 2003 with the ice edge located far north. Water discharge of the Lena and Kolyma Rivers was also below average level. The Kolyma River discharge in 2003 was similar to 2005,

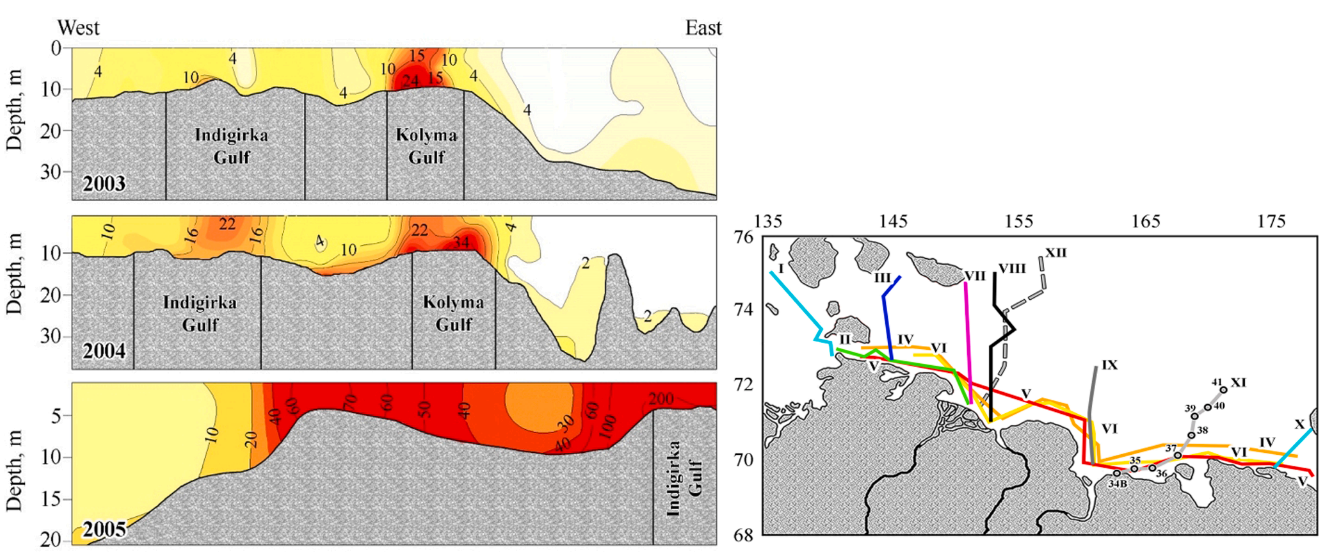

(a) (b)

Fig. 3. Vertical sections of the SPM (mg/L) (a). Positions of transects IV (orange), VI (yellow) and II (green) for 2003, 2004 and 2005, respectively (b).

Table 3
SPM data during 2000, 2003, 2004, 2005 and 2008.

Year	SPM	WBP		EBP		Total	
		surface	bottom	surface	bottom	surface	bottom
		n = 20		n = 17		n = 37	
2000	min–max	4.7–79.7	10.6–106.4	1.2–3.6	2.4–7.9	1.2–79.7	2.4–106.4
	mean ± s.d.	27.7 ± 22.3	30.1 ± 24.4	2.6 ± 1.4	4.6 ± 1.8	5.5 ± 1.8	17.4 ± 21.8
		n = 21		n = 23		n = 44	
2003	min–max	0.57–17.7	1.7–29.0	0.1–2.4	1.2–4.1	0.1–17.7	1.2–29.0
	mean ± s.d.	5.1 ± 4.5	7.8 ± 6.5	0.8 ± 0.9	2.4 ± 1.0	4.1 ± 3.7	6.7 ± 5.6
		n = 53		n = 32		n = 85	
2004	min–max	0.6–29.0	3.6–74.1	0.2–1.8	0.9–6.2	0.2–29.0	0.9–74.1
	mean ± s.d.	8.7 ± 7.3	15.5 ± 14.7	0.9 ± 0.3	2.4 ± 1.3	4.5 ± 6.3	9.1 ± 12.6
		n = 52					
2005	min–max	1.7–242.0	2.4–289.0	–	–	–	–
	mean ± s.d.	28.2 ± 50.4	32.2 ± 47.4	–	–	–	–
		n = 27		n = 33		n = 60	
	min–max	0.1–6.5	0.4–5.6	0.1–6.0	0.1–4.0	0.1–6.5	0.1–5.6
2008	mean ± s.d.	2.8 ± 2.5	1.5 ± 2.0	1.7 ± 2.9	2.3 ± 1.3	2.3 ± 2.7	1.9 ± 1.6
	Depth > 50 m (n = 1–2)						
	min–max	0.1–0.2	0.3	0.3	0.2–2.8	0.1–0.3	0.2–2.8

SPM – suspended particulate matter (mg/L); T – water temperature (°C); S - water salinity (‰); n – number of samples; mean – median content; s.d. – median absolute deviation; WBP - Western biogeochemical province; EBP - Eastern biogeochemical province.

but lower than the long-term average by 17.2 km^3 annually (17 %). The Yana River discharge was estimated as 32 km^3 which is equal to its annual average. Even with a low water discharge, the river plumes with S > 15 ‰ moved north beyond the Kolyma and Indigirka Gulfs. This translocation was promoted by winds. The position of the 25 ‰ isohaline in the surface waters, which is considered as a boundary of the mixing waters in the Arctic Seas, shifted almost 400 km to the east (to the Long Strait) compared to 2000. This might indicate an intensification of the SCC in 2003. Accelerating western transfer also caused increasing temperature of the surface waters. Meanwhile, the 0° isotherm of the bottom waters shifted significantly to the west.

The SPM content in September 2003 varied between 0.6 and 17.7 mg/L in the surface waters and 1.7 and 29.0 mg/L at the near bottom in the WBP. Calm and stable weather conditions led to much lower average SPM concentrations (five times lower in the WBP and two times lower in the EBP), if compared to 2000. The highest SPM values were observed near the Chukochy Cape, the Kolyma Gulf (Fig. 1). The SPM concentrations in the deltas of the large ESS rivers did not exceed 10 mg/L. This might point to a weakening of the ICD contribution to the Indigirka River waters. The main factor that limited the Kolyma River plume spreading out through the delta in 2003 seemed to be an intensification of the SCC, which pushed the river discharge along the coastline. Across the greatest part of the ESS, SPM concentrations in the bottom waters were twice those of the surface waters. This distinct vertical distribution of SPM might occur as a result of stratification, which led to accumulation of SPM in the bottom layers due to sedimentation processes (Table 3; Figs. 2, 3, S2, S3).

September 2004. Weak southern and southwestern winds were dominated over the WBP (WT regime) resulting in low wave action and more pronounced SCC comparing to 2003. In the EBP, the waves were slightly higher. The ice edge approached the coastline up to the 30 m isobath. Water with S < 20 ‰ reached the meridian of the Chaun Gulf for the first and only time during the observations. The freshening was also amplified by the increased river discharge in 2004. The discharge of the Kolyma River exceeded the long-term average by 17.4 km^3 (17 %), but was lower than 2003 by 34.6 km^3 (35 %). Off-shore winds distributed the relatively warm and fresh water towards the north. In delta front waters, the S decreased to 8–9 ‰ and the temperature exceeded 5 °C. The surface geostrophic currents indicate water transfer from the east to the west.

Two peaks of SPM content were detected in the ESS (Figs. 2, 3). They were formed from a single source – the erosion of ICD located along the WBP coasts. SPM concentrations varied from 0.6 to 29.0 mg/L and from 3.6 to 74.1 mg/L in the surface and bottom waters of the WBP, respectively. The weighted-average SPM content as well as its spatial and vertical distribution appeared similar to those in 2003. Offshore winds pushed the Indigirka River plume north beyond the gulf into the ESS. Sedimentation processes at the delta front slowed down presumably resulting in the relatively high SPM estimated at 28 mg/L (three times as high as in 2003). Outside the hydrological front (60–70 km from the delta front), the SPM content is reduced by half. SPM varied between 10.1 and 21.4 mg/L in the surface waters nearby the eroding permafrost coasts of the New Siberian Islands. The doubling of SPM concentrations in the bottom layer (15.6–33.6 mg/L) probably reflects active sediment resuspension caused by wind and tidal-induced wave action.

At 20–30 km away from the Kolyma Delta the content did not exceed 10 mg/L. Increase to 30–74 mg/L was forced away from the shallow of the Chukochy Cape. The maximum changes in SPM content occured with S values < 15 ‰. This indicates that removal of particles was controlled not only by intensive sinking, but also by biogeochemical transformation of OM (this is discussed further below). In the EBP, SPM concentrations ranged from 0.2 to 1.8 mg/L in the surface waters and between 0.9 and 6.2 mg/L in the bottom waters. Increase of SPM content up to 6.2 mg/L near the bottom might be explained by gravitational processes acting on the slopes of the Kolyma Paleovalley. Furthermore, the high content was found in a density layer of cold bottom waters. The SCC water flow was only traceable by TS-characteristics (T = 2–3 °C, S = 22–23 ‰) (Table 3; Figs. 2, 3, S2-S5).

September 2005. Field studies were carried out in the WBP only. The region was dominated by an ET regime, with about 70 % of the ice-free area by early September. Moderate eastern winds led to wave heights of 1.5–2.5 m (swell prevailed) causing mixing of the water masses and limited vertical variability of the SPM content in the water column. The Lena River discharge was estimated as 596 km^3 in 2005, which is 11 % higher than the annual average. The increase in discharge in 2004 compared to 2003 was 115 km^3 and another 38 km^3 in 2005 (this is 19 % higher than the annual average flow of the Yana River and less than of the Indigirka River by 35 %) (Table 2). River discharge constantly increasing over three years affected also the distribution of TS-parameters in the ESS, i.e. the area of warmer and fresher water expanded significantly to the north. The temperature distribution in the WBP in 2005 was the same as in 2000. In the shallow and mixed waters, T values did not exceed 3.8 °C and S fluctuations fell within the range of 12.8–23.3 ‰. The SPM content varied between 1.7 and 242.0 mg/L in the surface waters and between 2.4 and 289.0 mg/L in the near bottom waters. These increased SPM values resulted from both accelerated coastal erosion and more active resuspension of bottom sediments. This SPM distribution was associated with the WBP bottom relief. A series of relict swells were traced parallel to the coastline (cf. Aibulatov, 2001). The areas of increased SPM content are associated with the sediment resuspension from the edge of the swells, and a low content is traced over the inter-swell troughs. The SPM content also decreased with increasing distance from the shore, i.e. away from the epicenter of wave-induced turbidity and coastal ICD. The SPM content in the nearshore mixed water (S < 13 ‰) was up to 145–169 mg/L, whereas the more saline shelf waters (S ~ 20 ‰) beyond the SCC are characterized by lower SPM content varying between 5.2 and 6.7 mg/L. Horizontal SPM gradients ranged from 2.1 to 6.0 mg/L /km. The shallow regions (southeast of the New Siberian Islands) are characterized by strong resuspension induced by tidal energy (Dudarev et al., 2006a,b, 2008, 2015). The current velocity in this area can exceed 100 cm/s (Navigation book, 1998). In 2005, we observed SPM maxima of 42 to 289 mg/Land horizontal SPM gradients of 3.8 to 6.5 mg/L/km. Within this high tidal energy area, which is also characterized by a strong vertical stratification, the SPM content was > 30 times than outside this area. Continuous storm surges caused wave agitation at the depths of 20–25 m, which affected the entire water column and caused high turbidities and bottom resuspension (Table 3; Figs. 2, 3, S2, S3, S6-S8).

September 2008. We were able to carry out sampling across the entire ESS shelf and adjacent slope. The region was affected by an ET regime. The ice boundaries were located north of 80°N at some parts of the ESS (Ivanov et al., 2013; https: https://www.aari.nw.ru) (Fig. 1). River runoff far exceeded the average between the years 1936 to 2000 for the Lena River (705 km^3 compared with 535 km^3) and the Yana River (50 km^3 compared with 32 km^3). The Kolyma River discharge was lower than in 2004, but exceeded the long-term average by 11.1 km^3 (11 %). Despite higher river runoff in the Laptev Sea and a drop in S values by 7 to 10 ‰ below the annual average, we did not observe anomalies in S values of the ESS. The 30 ‰ isohaline was located along the isobathic line 120–140 m, i.e. it was spatially confined by the continental shelf. The ESS water masses were largely stratified. In the more mixed delta front, S values reached minima of ~ 18 ‰, while T values did not exceed ~ 6 °C (Figs. S2, S3).

The SPM in the outer shelf surface waters fluctuated from 0.1 to 1.0 mg/L. The SPM content in surface waters of the inner and middle shelf varied between 0.1 and 6.5 mg/L, while near the bottom it ranged from 0.1 to 5.6 mg/L. Stable conditions also led to a limited supply of sedimentary material from the nearshore zone; the maximum SPM content of 6.5 mg/L is recorded in the Indigirka River delta front and values of around 3 mg/L were found close to the coastal ICD sites in the Kolyma Gulf. At the outer shelf, content ranged from 0.1 to 0.3 mg/L (n = 2), in the surface waters and from 0.2 to 2.8 mg/L near the bottom. The horizontal variability of SPM content in the WBP and EBP was minimal and ranged between 0.1 and 6.5 mg/L. This can be attributed to low wave agitation heights (wave height about 1 m) and limited sediment resuspension. To the north of the continental slope, the SPM values were higher; this might be associated with phytoplankton growth. The content varied in a range of 2.1–2.8 mg/L in the surface waters and of 2.4–4.3 mg/L near the bottom.

In 2008 river runoff was anomalously high and the entire ESS area was ice free. The area of water mixing extended to the north, and the SPM content was generally low. Along the river paleovalleys towards the coast, the inflow of shelf waters with a low content of SPM (<0.5 NTU, turbidimeter sounding data) was traced. The prevailing northeasterly winds limited the lateral transport SPM, which resulted in low SPM content across almost the entire ESS except the river estuaries (Figs. 2, S9, S10).

Summary of 2000, 2003, 2004, 2005, and 2008. The SPM distribution in 2000 was characterized by the following factors: (i) a strong hydrodynamic impact of waves on the surface silty sediments in the WBP; (ii) SPM transport in the EBP limited by the pack ice mass, and (iii) a specific sedimentation as a result of the SCC and the pacific waters interaction. SPM patterns observed in 2003 were characterized by a low fluvial runoff and wave perturbation. Low SPM levels likely reflect the weak hydrodynamic background. Increase of the content during this period was due to the mobilization of SPM by the SCC flow, which reached the Long Strait in 2003. Most of the fluvial SPM was deposited within the Indigirka and Kolyma Gulfs. In 2004, southern winds pushed the freshwater relatively far north and the SCC extended beyond the ESS to the Chukchi Sea. The SPM content was low and comparable to that observed in 2003. As in 2000 and 2003, maximum SPM content and coastal erosion rates were observed in the western Kolyma Gulf. The SCC waters limited the SPM transport beyond the Kolyma and Indigirka Gulfs, and contributed to the intensification of sedimentation along the coastline. The SPM content and ET hydrometeorological regime in 2005 was similar to those in 2000. For the first time, we observed that high SPM content are not only limited to the nearshore shallow areas but can also exist further away from the coast. This offshore decreasing content is controlled by geomorphologic features (coastline submarine bars) and water circulation regime. Extremely low SPM content observed in 2008 was probably caused by limited bottom resuspension and low export of coastal erosion products away from the coast. It is also evident that the river runoff did not play a substantial role in the SPM distribution beyond the biogeochemical gradient zones of the Indigirka and Kolyma Gulfs.

The transport of SPM to the ESS through the western Dmitry Laptev and Sannikov Straits is insignificant compared to its mobilization from local sources (e.g. ICD) induced by storm and waves (Fig. S11). Model calculations suggest that high SPM contents remobilized from the sea bottom in the shallow waters can persist in suspended form for up to 5–15 days, and most of this material (up to 90 %) is redeposited near the source (Kulakov, 2008). Thus, the SPM concentration of the SCC waters is controlled by weather conditions. Due to the constant removal of SPM from the SCC, the SPM content at the western border of the Chukchi Sea did not exceed the background values for coastal waters. Thus, in September 2003 (WT regime) the SPM content in the Long Strait was < 3 mg/L, and the SCC was characterized by T ~ 1.5° and S ~ 25 ‰. The waters above the opposite Wrangel Island slope were characterized by T > 0°, S ~ 28 ‰ and SPM content < 1.5 mg/L. In September 2003 and 2004 (WT regime), T and S values of the SCC increased even more (T ~ 3.0°, S = 22–23 ‰), but the SPM level did not change (Fig. 12S). Under favorable conditions (WT regime) of the SCC flow to the east, the SCC waters had low SPM content comparable to that of the adjacent seas. Hence, the SPM transit to the ESS via the SCC is limited. From outside the ESS, the SPM could enter the waters in both fine and subcolloidal fractions but in non-significant concentrations. It is therefore clear that satellite images showing yellow–brown colored clouds in the ESS coastal waters primarily indicate a colored dissolved OM (CDOM) enrichment, but not high SPM concentrations (Pugach et al., 2015, 2018; Pugach and Pipko, 2013; Charkin et al., 2015; Dudarev, 2016).

In ET regime-dominated years, cold arctic air weakens the thawing of ICD and stabilizes the permafrost sediments. However, the ICD material of the previous year still remains in the coastal zone. Surge winds intensify coastal erosion and transport large volumes of eroded material into the shelf waters. With winds from the mainland (WT regime), warm air enhances the thawing of ICD and, thus, enhances both thermal denudation and solifluction, while waves in the coastal zone are weakened. Such winds enforce the lateral transport of both SPM and river freshwater away from the shore, but it is still limited by the flow of the SCC. Most SPM is deposited within the narrow gradient zone between SCC and the runoff waters in the Indigirka and Kolyma Gulfs. A direct relationship was demonstrated between the wind regime and sedimentation in the coastal zone of Eastern Arctic Seas (Charkin et al., 2011, 2015; Dudarev, 2016; Sanchez-Garcia et al., 2014). Satellite imagery serves as a visualization of longshore transport of the SPM for years dominated by ET or WT hydrometeorological regimes (Fig. 4). Statistical analysis revealed correlations between the SPM, T and S values in the mixing areas of river and sea waters. While for the years 2003, 2005 and

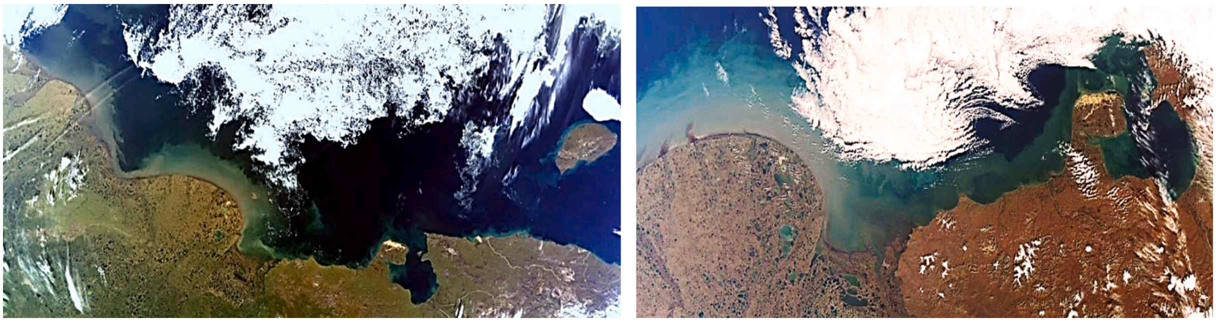

Fig. 4. SPM longshore fluxes with ET (left) and WT (right) regimes of hydrometeorological processes. Visible range of the MODIS spectroradiometer (http://rapidfire.sci.gsfc.nasa.gov).

2008 the correlation coefficient (R^2) was < 0.5, it was higher in 2000 (R^2 = 0.7–0.9) and in 2004 (R^2 = 0.5–0.7) (Fig. S13).

4.2. Intraannual variability of the SPM content

During the spring-summer flood in June, landfast ice begins to break down while the edge is still located near the coast. Most of the riverine SPM settles along this mechanical obstacle, which acts as a barrier for SPM. In August-September, the input of SPM weakens as the river flow weakens. It follows that the runoff waters distribute over a larger area and the SCC intensifies, as well as along shore and lateral transport of SPM. During this period, wind forcing becomes increasingly important for the sedimentation of the inner shelf. The intensity of wave energy regulates the degree of remobilization of material from the coastal slope and from isolated shallows. There is a clear relationship between the SPM content and the depth of the center of wave erosion. Our results indicate that the river paleovalleys do not play a significant role in the SPM offshore transport. By October, the river outflow weakens further. Ice formation begins in the shallow waters, and the sea ice begins to drift towards the coast. However, the SPM, as well as the sedimentary material remobilized by the autumn storms from the bottom, is deposited along the edge of the drifting ice and is partially incorporated into the sea ice.

4.3. Interannual variability of the elemental and isotopic signatures of particulate organic matter

4.3.1. Particulate organic carbon

The spatial distribution of POC (%) is contrary to the distribution of the SPM, which may be explained by dilution and sediment composition. The lowest POC contribution is observed in the areas of high SPM content close to shore. The middle and outer shelf areas were characterized by higher POC concentrations. The highest POC variability occured in the zones of river-sea water mixing in the Indigirka and Kolyma Gulfs. A similar distribution was observed in the Ob and Yenisey Rivers - Kara Sea, Lena River - Laptev Sea mixing zones (Dudarev et al., 2006a; Charkin et al., 2011; Kodina et al., 2009). The lower vertical variability in the WBP is also the result of water mixing. In the more stratified EBP, the POC content in the surface waters was almost 1.5 times higher than at the bottom, which is likely due to high plankton productivity in the euphotic zone (Table 4; Fig. 5).

4.3.2. Total nitrogen

In 2000–2008, the TN concentrations ranged between 0.02 and 12.2 % in the surface waters and between 0.02 and 7.90 % in the bottom waters of the WBP. In the EBP, the concentrations varied from 0.01 to 9.0 % and from 0.01 to 1.4 % in the surface and bottom waters,

Table 4
POC, TN and POC/TN data of SPM during 2000, 2003, 2004, 2005 and 2008.

Year	Statistical parameters	POC, %				TN, %				POC/TN			
		WBP		EBP		WBP		EBP		WBP		EBP	
		surface	bottom	surface	bottom	surface	bottom	surface	bottom	surface	bottom	surface	bottom
Depth < 50 *m*													
2000	min–max	0.9–18.9	0.8–18.8	2.0–42.9	1.3–40.1	0.03–0.2	0.03–0.2	0.01–0.2	0.01–0.2	7.7–13.1	8.0–12.4	5.5–10.4	5.5–10.0
	mean ± s.d.	8.3 ± 9.0	7.3 ± 8.0	24.3 ± 27.4	16.3 ± 25.2	0.1 ± 0.04	0.11 ± 0.04	0.1 ± 0.05	0.12 ± 0.05	10.1 ± 1.6	10.1 ± 1.4	7.8 ± 1.1	7.6 ± 1.0
2003	min–max	1.1–16.9	0.7–6.4	3.0–62.9	1.6–5.8	0.2–2.9	0.1–0.9	0.4–9.0	0.3–0.7	5.9–8.4	4.6–10.4	5.2–9.1	6.1–7.8
	mean ± s.d.	4.6 ± 3.6	2.9 ± 1.5	21.1 ± 22.6	3.9 ± 1.3	0.7 ± 0.6	0.4 ± 0.2	3.1 ± 3.2	0.6 ± 0.2	6.8 ± 0.6	7.0 ± 1.0	7.0 ± 1.1	6.7 ± 0.6
2004	min–max	2.5–44.0	1.6–11.0	0.1–25.9	3.9–13.8	0.06–2.0	0.05–0.6	0.1–2.3	0.2–1.4	6.7–16.6	5.5–10.6	5.5–10.5	6.2–9.6
	mean ± s.d.	8.2 ± 9.3	3.8 ± 1.7	12.7 ± 4.9	7.6 ± 2.9	0.4 ± 0.4	0.2 ± 0.1	0.9 ± 0.5	0.5 ± 0.3	9.3 ± 1.8	8.2 ± 1.0	7.4 ± 1.0	7.7 ± 0.9
2005	min–max	0.3–29.8	0.5–11.3	–	–	0.01–2.1	0.01–0.4	–	–	7.1–13.4	7.8–13.1	–	–
	mean ± s.d.	6.3 ± 7.0	3.5 ± 2.7	–	–	0.3 ± 0.4	0.2 ± 0.1	–	–	10.3 ± 1.6	10.6 ± 1.5	–	–
2008	min–max	0.2–49.1	0.2–15.5	0.8–17.7	1.7–6.1	0.02–12.2	0.01–7.9	0.2–3.1	0.3–1.2	3.8–8.1	4.8–7.8	4.7–6.0	4.9–7.8
	mean ± s.d.	9.8 ± 14.2	5.7 ± 5.1	6.8 ± 6.7	3.6 ± 1.7	2.2 ± 3.3	1.3 ± 1.7	1.3 ± 1.2	0.7 ± 0.4	5.5 ± 1.1	6.2 ± 0.8	5.4 ± 0.5	6.2 ± 0.9
Depth > 50 *m*													
2008	min–max	0.1–35.5	6.0–46.5	–	–	0.02–7.5	0.01–7.9	–	–	4.7–6.6	5.7–7.5	–	–
	mean ± s.d.	11.0 ± 16.7	21.4 ± 21.9	–	–	2.2 ± 3.6	2.7 ± 3.5	–	–	5.6 ± 0.8	6.3 ± 0.8	–	–
Entire shelf													
2000–2008	min–max	0.1–49.1	0.2–46.5	0.1–62.5	0.1–12.6	0.01–12.2	0.02–7.9	0.01–9.0	0.01–1.4	3.8–16.6	4.6–12.4	4.7–10.5	4.9–10.0
	mean ± s.d.	4.9 ± 8.0	3.3 ± 5.4	3.0 ± 10.8	10.7 ± 2.2	0.8 ± 1.8	0.5 ± 0.9	1.1 ± 1.6	0.4 ± 0.3	7.8 ± 2.2	7.7 ± 1.7	7.1 ± 1.3	7.3 ± 1.1

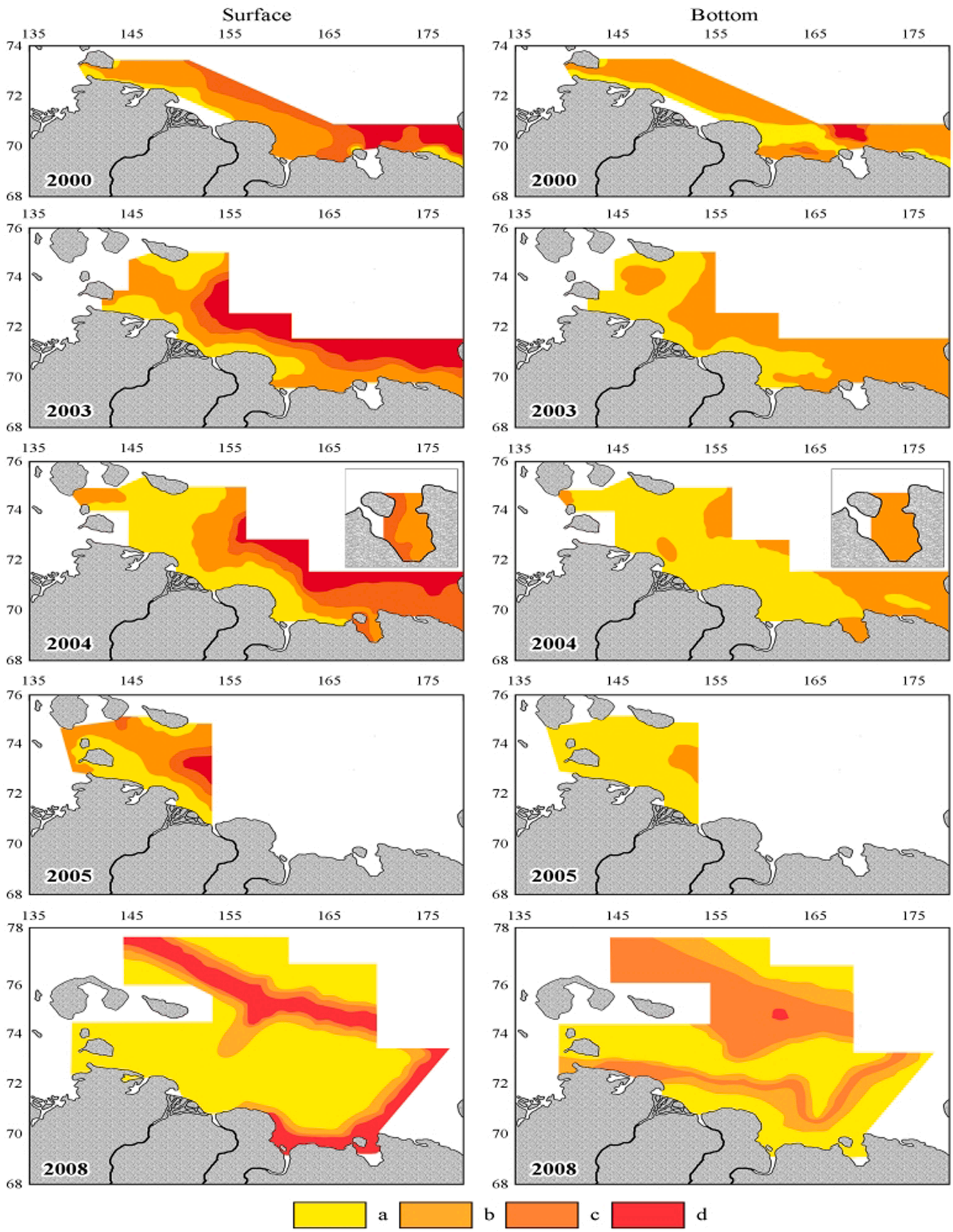

Fig. 5. POC content during 2000, 2003, 2004, 2005 and 2008. POC (%): a - < 5, b — 5–15, c — 15–25, d - > 25.

respectively. The weighted averages in 2003 and 2008 were exceptionally high (1.19 and 1.36 %, respectively) while values in 2000 were low (0.12 %).

The spatial distribution of TN changed over the years (Fig. 6). In 2000 we observed elevated values, which might be associated with the terrigenous input that dominated in the WBP. In the EBP, TN values generally increased to the east, which might reflect an increasing contribution of marine plankton as an important nitrogen source. The dominating hydrological regime was the ET, while an increased water inflow came from the Bering and Chukchi Seas into the ESS. A similar situation was also observed in 2005. In 2003, most of the ESS was characterized by high TN values which were mainly confined to depths > 20–25 m. A high TN content was also detected in the SPM of the SCC. The TN content decreased towards the bottom waters. The SPM in the

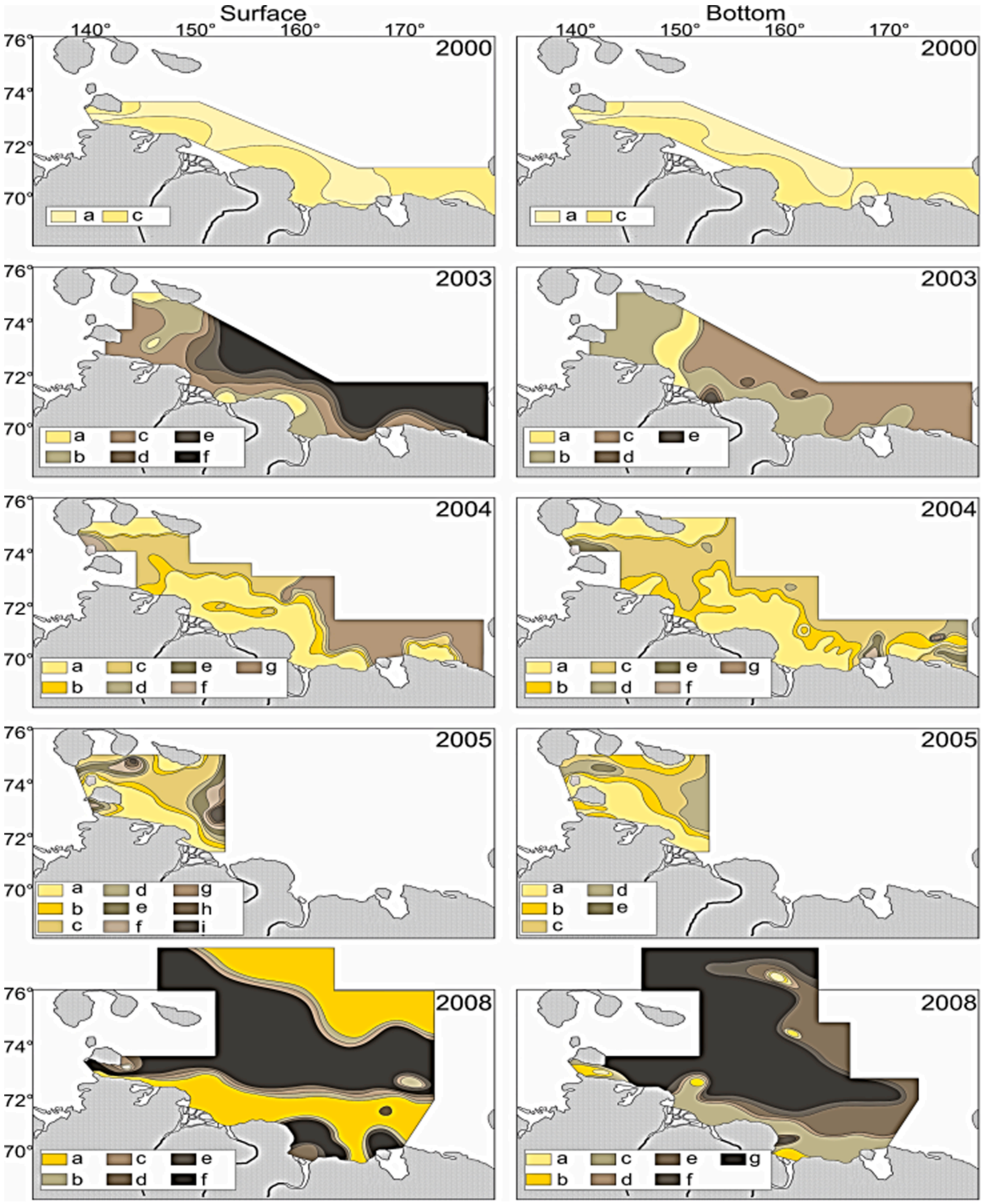

Fig. 6. TN content during 2000, 2003, 2004, 2005 and 2008. TN (%): *2000*. Surface: a – <0.1, b – 0.1–0.2. Bottom: same. *2003*. Surface: a – 0.1–0.3, b – 0.3–0.5, c – 0.5–0.7, d – 0.7–0.9, e – 0.9–1.1, f - >1.1. Bottom: a – 0.1–0.3, b – 0.3–0.5, c – 0.5–0.7, d – 0.7–0.9, e – 0.9–1.1. *2004*. Surface: a – <0.1, b – 0.1–0.2, c – 0.2–0.3, d – 0.3–0.4, e – 0.4–0.5, f – 0.5–0.6, g - >0.6. Bottom: same. *2005*. Surface: a – <0.1, b – 0.1–0.2, c – 0.2–0.3, d – 0.3–0.4, e – 0.4–0.5, f – 0.5–0.6, g – 0.6–0.7, h – 0.7–0.8, i - >0.8. Bottom: a – <0.1, b – 0.1–0.2, c – 0.2–0.3, d – 0.3–0.4, e – <0.4. *2008*. Surface: a – <0.3, b – 0.3–0.5, c – 0.5–0.7, d – 0.7–0.9, e – 0.9–1.1, f – >1.1. Bottom: a – <0.1, b – 0.1–0.3, c – 0.3–0.5, d – 0.5–0.7, e – 0.7–0.9, f – 0.9–1.1, g – >1.1.

bottom waters was characterized by a low TN content in the Indigirka and Kolyma Rivers paleovalleys. In 2004, the area with low TN contents significantly expanded with its minima in the estuaries of the Indigirka and Kolyma Rivers. In 2008, the highest TN contents with an unusual spatial distribution were observed. The SPM at the middle shelf was characterized by a TN maximum, as well as the Kolyma Gulf and the area along the Chaun Gulf. The lowest TN contents were found on both outer and inner shelf, with concentrations of < 0.01 % on the outer shelf. The thermohaline circulation resulted in a vertical stability of the water column here, which affected the downwelling of the surface waters with a low TN content. The SPM in the bottom waters of the SCC is also characterized by low TN values (Table 4; Fig. 6).

4.3.3. POC/TN ratio

POC/TN ratios for the period 2000–2008 ranged between 3.8 and 16.6 in the surface waters and between 4.6 and 12.4 near the bottom in the WBP, and between 4.7 and 10.5 and 4.9–10.0 in the EBP, respectively. The weighted mean values for the surface and bottom waters were comparable. For the 2000–2005 period, the POC/TN ratios exceeded 10, while the highest POC/TN ratio did not exceed 8.1 in 2008 (Table 3; Fig. 7).

4.3.4. Stable carbon isotopes

In 2000–2008, the $\delta^{13}C$ values varied between –32.4 - −25.2 ‰ in the surface waters and between − 29.4 - −24.9 ‰ near the bottom in the WBP. In the EBP, the carbon isotope signatures ranged between − 28.9 -

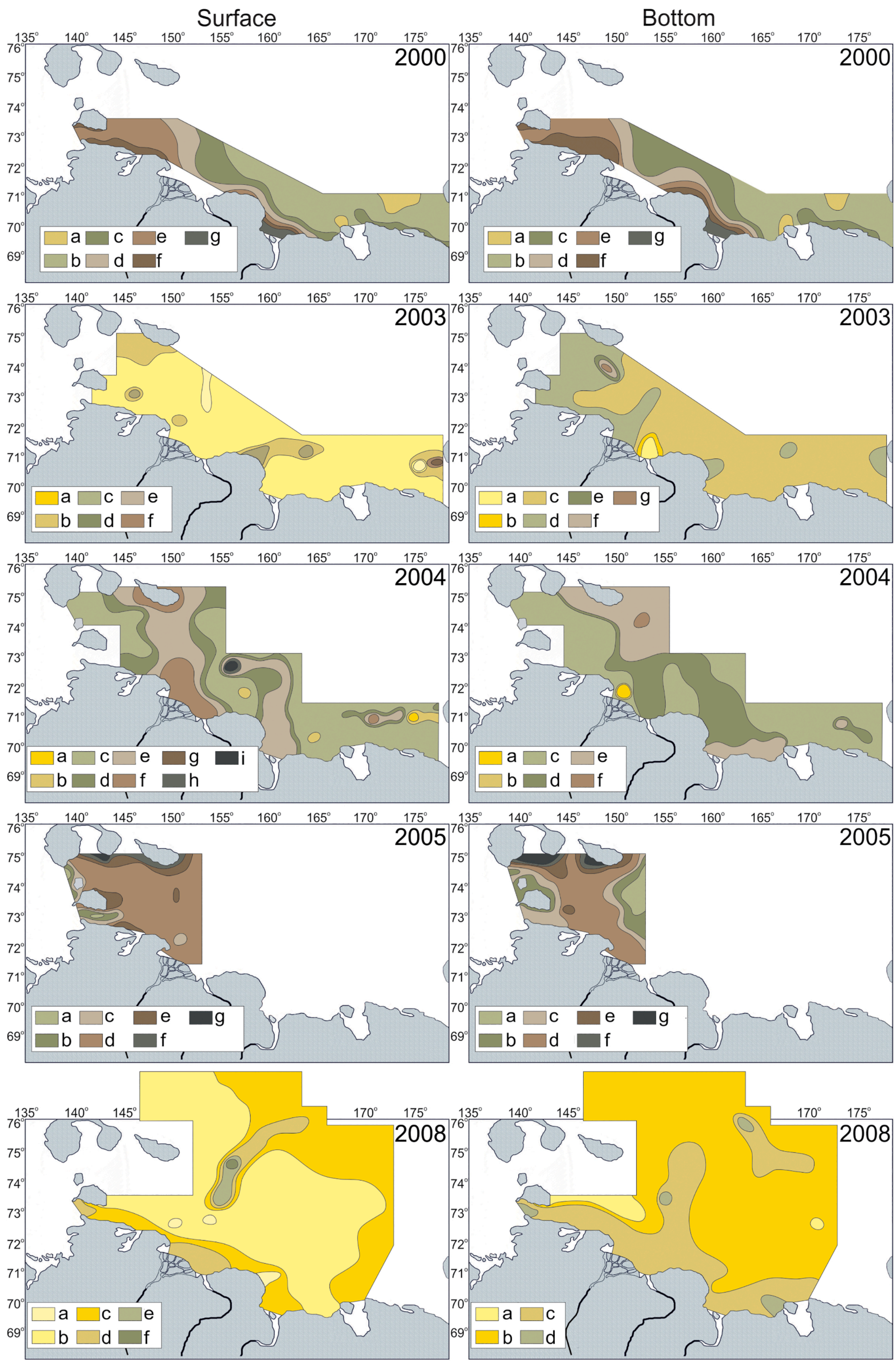

Fig. 7. POC/TN ratio during 2000, 2003, 2004, 2005 and 2008. POC/TN ratio: 2000. Surface: a – 6÷7, b – 7÷8, c – 8÷9, d – 9÷10, e – 10÷11, f – 11÷12, g – 12÷13. Bottom: same.2003. Surface: a – 5÷6, b – 6÷7, c – 7÷8, d – 8÷9, e – 9÷10, f – >10. Bottom: a – 4÷5, b – 5÷6, c – 6÷7, d – 7÷8, e – 8÷9, f – 9÷10, g – >10.2004. Surface: a – 5÷6, b – 6÷7, c – 7÷8, d – 8÷9, e – 9÷10, f – 10÷11, g – 11÷12, h – 12÷13, i – >13. Bottom: a – 5÷6, b – 6÷7, c – 7÷8, d – 8÷9, e – 9÷10, f – 10÷11.2005. Surface: a – 7÷8, b – 8÷9, c – 9÷10, d – 10÷11, e – 11÷12, f – 12÷13, g – 13÷14. Bottom: same.2008. Surface: a – 3÷4, b – 4÷5, c – 5÷6, d – 6÷7, e – 7÷8, f – 8÷9. Bottom: a – 4÷5, b – 5÷6, c – 6÷7, d – 7÷8.

–23.4 ‰ and between − 28.5 - –23.2 ‰, respectively. The lowest $\Delta\delta^{13}C$ (differences between lowest and highest values) variability was observed in 2000 ($\Delta\delta^{13}C$ = -2.7 ‰), 2003 ($\Delta\delta^{13}C$ = -3.5 ‰) and 2005 ($\Delta\delta^{13}C$ = -2.0 ‰). A wider range of $\Delta\delta^{13}C$ values was recorded in 2004 ($\Delta\delta^{13}C$ = -4.3 ‰) and maximized in 2008 ($\Delta\delta^{13}C$ = -5.0 ‰; $\Delta\delta^{13}C$ = -8.1 ‰ on the middle and outer shelf). In the WBP, $\delta^{13}C$ values varied from –32.4 ‰ to − 27.4 ‰ (on the outer shelf up to − 24.3 ‰). A similar $\Delta\delta^{13}C$ variability was observed in the EBP. However, in 2008, the values ranged between − 28.9 and –23.0 ‰ ($\Delta\delta^{13}C$ = -5.9 ‰) on the inner and middle shelf of the EBP and − 31.6 - −21.8 ‰ ($\Delta\delta^{13}C$ = -9.8 ‰) on the

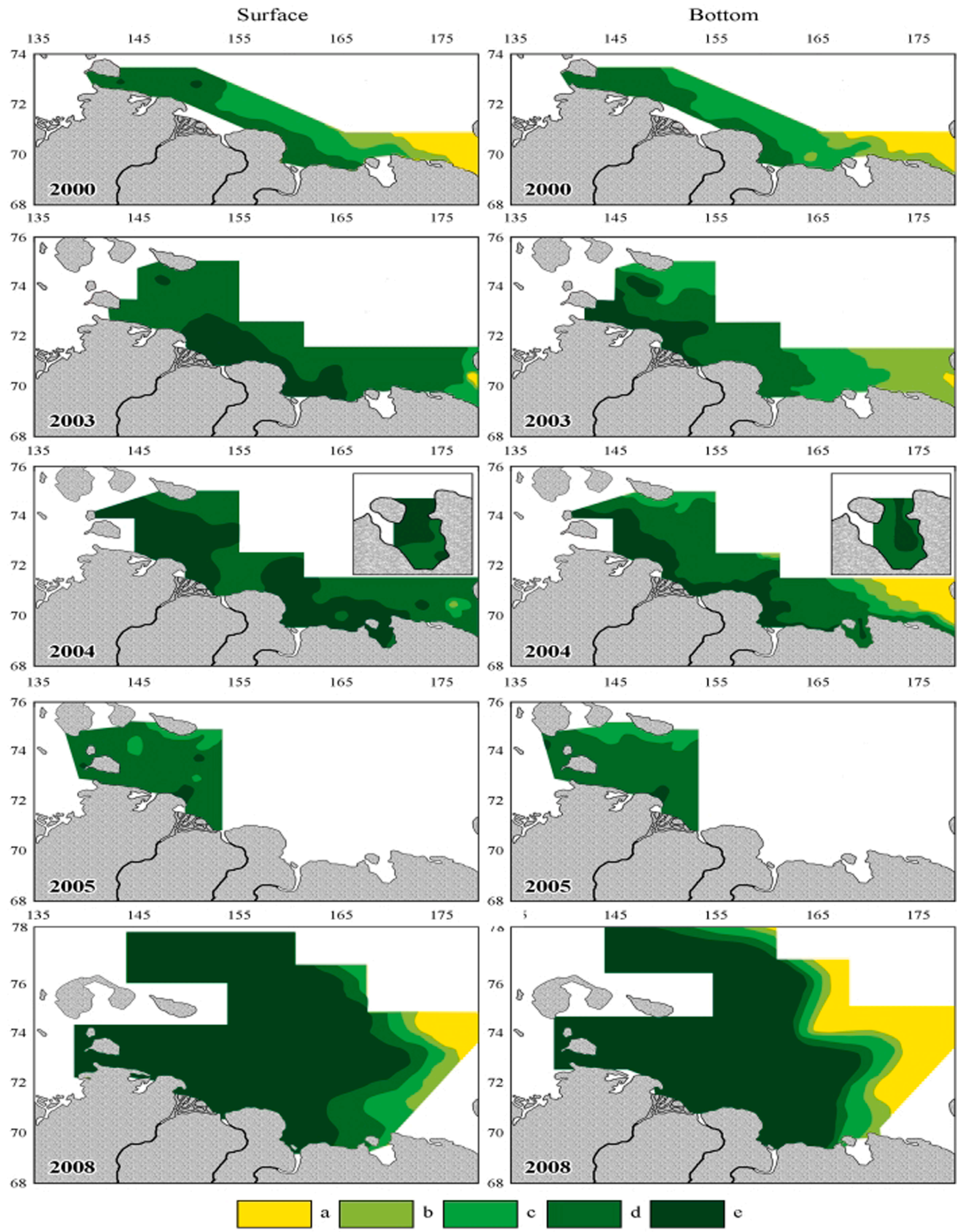

Fig. 8. $\delta^{13}C$ POC values during 2000, 2003, 2004, 2005 and 2008. $\delta^{13}C$ (‰): a - >-24, b - −25 - −24, c - −26 – −25, d - −27 - −26, e - <-27.

outer shelf. In 2000–2008, the $\delta^{13}C$ values varied from –32.4 to – 21.8 ‰ with $\Delta\delta^{13}C$ = -10.6 ‰ (Table 4; Fig. 8).

4.3.5. Nitrogen stable isotopes

In 2000–2008, $\delta^{15}N$ values were between – 0.9–14.6 ‰ in the surface waters and between 3.3 and 14.2 ‰ near the bottom in the WBP. In the EBP, those varied between 4.5 and 14.1 ‰ and 1.1–10.6 ‰, respectively. The longterm average for $\delta^{15}N$ in 2000–2008 was 6.4 ‰ for the entire ESS (6.0 and 7.6 ‰ for the WBP and the EBP, respectively). In 2008, $\delta^{15}N$ extreme values were – 0.9 and 14.2. Furthermore, there were no clear differences in $\delta^{15}N$ values between the surface and bottom waters (Table 5; Fig. 9).

4.3.6. Possible sources of POC

As discussed above, the interannual variability of the SPM content in the ESS depends on (i) the intensity of coastal erosion of ICD; (ii) the volume of river runoff; and (iii) the prevailing ice and wind regime. We also identified a direct connection between the wind regime and periods of activation and weakening of sedimentary processes in the near-coastal area. Two hydrometeorological regimes (upwind and down-wind) can be distinguished, that drive the preparation and removal of thermal abrasion products to the sea (Charkin et al., 2011, 2015; Dudarev, 2016). Areas of maximum SPM content are confined to the mouths of large rivers and along the widespread thermal abrasive coastlines. Hence, SPM formes a structure that encircles the land, which is the most strongly developed in the WBP. The contents rapidly decrease outside shallow waters and runoff plumes. By contrast, there is an increase in POC content in the EBP. The EBP is influenced by the advection of the Chukchi Sea waters enriched in biogenic elements (Savelyeva et al., 2008). Due to strong primary production, surface waters are undersaturated in carbon dioxide relative to the atmospheric content (Anderson et al., 2011; Pipko et al., 2005, 2011). The total carbon sequestration by primary production of phytoplankton (including the production of cryophilic phytoplankton) is for the EBP estimated at 18.5 mg C/m^2 per day. This value is comparable to the Laptev Sea, but only half of that in the adjacent Chukchi Sea (Vetrov and Romankevich, 2011). Diatoms account for up to 90 % of the planktic POC production in the Arctic seas (Vinogradov et al., 2001). Freshly synthesized OM of algae is poorly resistant to oxidative diagenesis and is almost completely utilized and transformed into labile bacterial proteins (Vetrov and Romankevich, 2004).

Elemental isotopic and molecular markers are useful to identify relative source contributions to the POC pool. Table 5 presents the elemental and isotopic markers of ICD coastal slope, SPM and bottom sediments of the Dmitry Laptev Strait. > 95 % of the coastline of the strait is composed of ICD, while the strait acts as a transit system for the transfer of sedimentary and OM between adjacent seas. It is thus possible to observe the transformation of the initial biogeochemical SPM signal during the water transport. The POC/TN ratio is used to estimate the ratio of the contribution of terrigenous and marine sources to the POC. For terrestrial OM, values typically range from 15 to 20, and for marine OM from 6 to 7 (Galimov, 1981; Vetrov et al., 2008; Stein and Nurnberg, 1995; Semiletov, 1999). In the 2000–2008 data set the range of POC/TN ratios was 3.8–17.6. At the annual scale, the spatial distribution pattern of POC/TN variability is also highly heterogeneous (Fig. 7).

The endmember POC/TN value of the coastal ICD in the Dmitry Laptev Strait is 11.3–13.4 (Table 6), while for SPM it is between 7.5 and 9.7, which is due to biogeochemical transformation of the OM. The transformation starts onshore after the ICD material has thawed and eroded material remains as so-called thaw slumps on the beach until the thermal abrasion products are washed into the sea and transferred to SPM-POC by frequently-occuring storm events. Already in the stage of

Table 5

$\delta^{13}C$, $\delta^{15}N$ and terrOC data of SPM during 2000, 2003, 2004, 2005 and 2008.

Year	Statistical parameters	$\delta^{15}N$, ‰				$\delta^{13}C$, ‰				TerrOC, %			
		WBP		EBP		WBP		EBP		WBP		EBP	
		surface	bottom	surface	bottom	surface	bottom	surface	bottom	surface	bottom	surface	bottom
Depth < 50 *m*													
2000	min–max	3.2–6.3	3.3–6.2	5.0–8.3	4.9–9.7	−27.6-−25.2	−26.8-−24.9	−25.3-–23.4	−25.1-–23.2	34–75	33–77	1–10	1–10
	mean ± s.d.	4.5 ± 0.8	4.5 ± 0.8	7.2 ± 0.9	7.3 ± 1.1	−26.3 ± 0.6	−26.2 ± 0.6	−24.2 ± 0.8	−24.1 ± 0.8	54 ± 9.8	54 ± 10.3	24 ± 12.1	23 ± 11.3
2003	min–max	3.3–8.0	3.4–12.0	5.6–12.9	6.6–8.4	−27.9-−25.6	−29.1-−25.7	−26.7-−24.0	−25.1-–23.8	45–94	46–76	21–60	18–37
	mean ± s.d.	5.3 ± 1.1	5.2 ± 1.7	8.0 ± 1.9	7.2 ± 0.6	−26.9 ± 0.7	−26.6 ± 0.5	−25.7 ± 0.9	−24.5 ± 0.5	67 ± 10.2	59 ± 8.3	46 ± 13.1	28 ± 7.2
2004	min–max	1.1–7.8	4.6–8.1	4.5–10.9	5.5–9.3	−29.2-−25.6	−28.4-−24.9	−27.7-−24.1	−28.4-–23.4	44–99	33–87	22–76	12–86
	mean ± s.d.	5.6 ± 1.5	6.4 ± 0.9	7.6 ± 1.4	7.4 ± 0.9	−27.3 ± 0.8	−26.8 ± 0.7	−26.6 ± 0.7	−25.9 ± 1.4	70 ± 11.2	64 ± 10.0	60 ± 11.1	49 ± 20.7
2005	min–max	2.0–11.6	2.4–12.5	–	–	−27.4-−25.6	−27.1-−25.4	–	–	42–73	42–66	–	–
	mean ± s.d.	6.5 ± 2.6	6.2 ± 2.1	–	–	−26.4 ± 0.5	−26.2 ± 0.5	–	–	56 ± 7.9	53 ± 7.7	–	–
2008	min–max ьфч	−0.9–14.7	3.3–14.2	4.5–14.1	1.1–10.6	–32.4-−27.5	−29.4-−27.4	−28.9-–23.5	−28.5-–23.0	57–88	54–74	22–84	18–69
	mean ± s.d.	6.0 ± 4.2	6.1 ± 2.0	7.8 ± 3.0	7.4 ± 2.9	−29.8 ± 1.3	−28.2 ± 0.7	−27.1 ± 1.5	−25.9 ± 1.9	75 ± 8.9	63 ± 6.3	53 ± 16.6	40 ± 16.9 9
Depth > 50 *m*													
2008	min–max	6.0–10.0	6.5–10.2	–	–	–32.4-−28.4	−24.7-−24.3	−30.6-−27.6	−31.6-−21.8	65–100	32–72	58–84	3–93
	mean ± s.d.	8.2 ± 1.6	8.9 ± 1.6	–	–	−30.4 ± 2.0	−24.5 ± 0.3	−29.4 ± 1.3	−27.2 ± 4.2	82 ± 17.6	50 ± 20.3	71 ± 10.8	37 ± 41.8
Entire shelf													
2000–2008	min–max	−0.9–14.6	3.3–14.2	4.5–14.1	1.1–10.6	−32.4-−25.2	−29.4-−24.9	−28.9-–23.4	−28.5-–23.0	34–99	33–87	1–84	1–86
	mean ± s.d	5.9 ± 2.5	6.1 ± 2.0	7.8 ± 1.8	7.4 ± 1.3	−27.3 ± 0.8	−26.8 ± 0.6	−25.9 ± 1.0	−25.1 ± 1.2	64 ± 9.6	59 ± 8.5	46 ± 13.2	35 ± 14.0

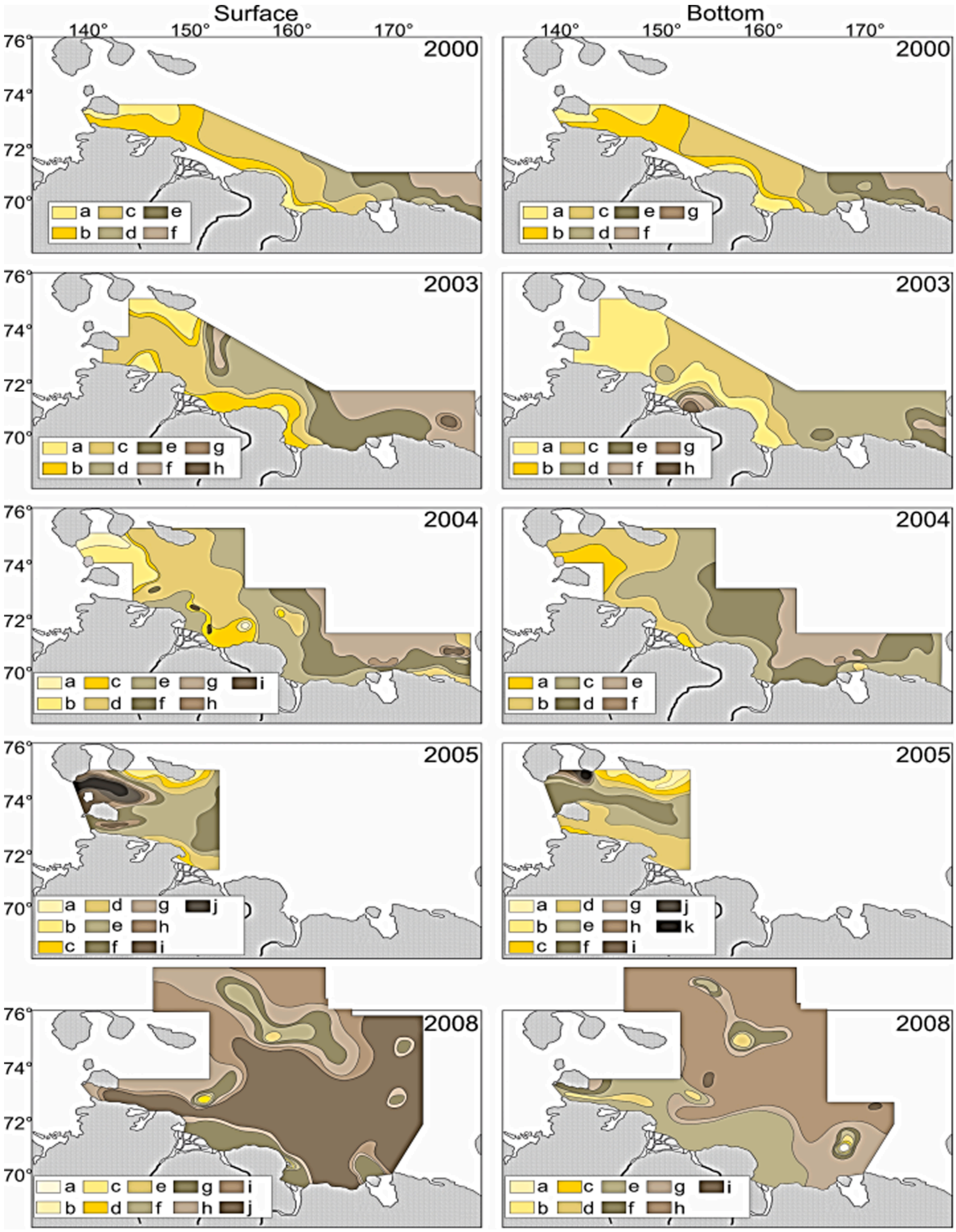

Fig. 9. δ^{15}N value during 2000, 2003, 2004, 2005 and 2008. δ^{15}N (‰): 2000. Surface: a – 3÷4, b – 4÷5, c – 5÷6, d – 6÷7, e – 7÷8, f – 8÷9. Bottom: a – 3÷4, b – 4÷5, c – 5÷6, d – 6÷7, e – 7÷8, f – 8÷9, g – 9÷10. 2003. Surface: a – 3÷4, b – 4÷5, c – 5÷6, d – 6÷7, e – 7÷8, f – 8÷9, g - 9÷10, h >10. Bottom: same.2004. Surface: a – <3, b – 3÷4, c – 4÷5, d – 5÷6, e – 6÷7, f – 7÷8, g – 8÷9, h – 9÷10, i – >10. Bottom: a – 4÷5, b – 5÷6, c – 6÷7, d – 7÷8, e – 8÷9, f – 9÷10.2005. Surface: a – <3, b – 3÷4, c – 4÷5, d – 5÷6, e – 6÷7, f – 7÷8, g – 8÷9, h – 9÷10, i – 10÷11, j – 11÷12. Bottom: a – <3, b – 3÷4, c – 4÷5, d – 5÷6, e – 6÷7, f – 7÷8, g – 8÷9, h – 9÷10, i – 10÷11, j – 11÷12, k – >12.2008. Surface: a – -1÷0, b – 0÷3, c – 3÷4, d – 4÷5, e – 5÷6, f – 6÷7, g – 7÷8, h – 8÷9, i – 9÷10, j – >10. Bottom: a – <3, b – 3÷4, c – 4÷5, d – 5÷6, e – 6÷7, f – 7÷8, g – 8÷9, h – 9÷10, i – >10.

thaw slumps, the POC/TN ratio decreases to ca. 8.9 while the OC content decreases significantly, down to one order of magnitude less compared to the POC (Dudarev et al., 2003; 2006a). In general, there is usually a transition in the main OC source for POC, from terrigenous-dominated to a mixed and marine source from the west to the east of the ESS. This was the case in 2000 and 2005, when the POC/TN values were 8.7–11.3 in the WBP. By contrast, in 2003 the signal of the marine POC dominated, with ratios between 6 and 7. POC/TN ratios in 2008 (as well as for POC and TN) were yet lower with values from 4 to 6, while in river-influenced gulfs and on the middle and outer shelf values were between 6 and 7, and on the outer shelf between 5 and 6. In the shallow areas outside the Indigirka River Paleovalley (25 m depth), values were as low as 3–4. This may be related to an assumed vortex-like vertical thermohaline circulation that occurred in this area in 2008. The circulation formed at the apex of the salt intrusion of shelf waters and facilitated the upwelling of salty and low-temperature bottom waters to the surface. Such conditions are characterized by an oxygen deficiency and an increased content of mineral forms of nitrogen (Savelyeva et al.,

Table 6
Elemental and isotopic markers of the coastal ICD, SPM and bottom sediments (BS) in the Dmitry Laptev Strait.

Parameters	Coastal ICD	SPM		BS	Average		
		surface	bottom		coastal ICD	POC	BS
OC, %	2.5–3.5	–	–	0.1–1.6	3.1	–	0.6
POC, %	–	0.13–1.68	0.11–2.25	–	–	0.71	–
TN, %	0.22–0.28	0.01–0.21	0.01–0.28	0.07–0.14	0.25	0.08	0.09
POC/TN	11.3–13.4	7.5–8.8	7.6–9.7	11.8–12.9	12.4	8.1	12.7
δ^{13}C, ‰	−27.2 - −26.4	−27.5 - −26.3	−27.1 - −25.8	−27.1 - −26.6	−26.9	−26.8	−26.8
δ^{15}N, ‰	−0.49–3.83	3.3–6.8	4.5–5.5	3.7–4.7	1.7	4.9	4.9
terrOC, %	100	90–100	90–98	76–100	100	95	85

2008). The content of TN and POC reached 2.0 and 7.6 %, respectively.

The δ^{13}C isotopic signature was also used to elucidate the origin of POC (see Supplementary Results and discussion S2). The δ^{13}C values ranged from –32.4 to − 21.8 ‰ in 2000–2008 which suggests a variety of POC sources and water masses as well as species composition of plankton communities, and ongoing biochemical transformations of OM in both the drainage basin and during oceanic water mass transport. The δ^{13}C of the Indigirka Gulf POC was − 27.8 - −26.5 ‰ during 2000–2005. Similar values were published for Kolyma, Mackenzie, Yukon and Colville Rivers (Vonk et al., 2010; Vonk and Gustafsson, 2013; Sanchez-Garsia et al., 2011). The POC that forms to the east of the Kolyma Gulf, is isotopically heavier. The average difference in the δ^{13}C signatures between allochtonous (fluvial) and autochthonous (marine) plankton is − 9 ‰ and may be explained by discrimination of the heavy ^{13}C during photosynthesis. The enrichment of the ^{13}C in the seawater carbonate system provided by accumulation of the bicarbonate ion leads to a yet higher isotope ^{13}C content in marine OM (Galimov, 1981). The low δ^{13}C value of − 21.8 ‰ along with the lowest POC/TN ratio of 6.5 was observed on the outer shelf of the ESS. In 2000 and 2008, during the ET regime setting, the gradient zone between terrigenous and marine-dominated POC was approximately along the 165° E. This location was previously shown to be a hydrological and biogeochemical gradient frontal zone between the WBP and EBP waters (Semiletov et al., 2005; Pipko et al., 2011). As a result of the SCC intensification (2003, 2004), the gradient zone shifted hundreds of kilometers to the east. In 2003 it reached the Long Strait, and in 2004 it moved to the Chukchi Sea (Fig. 8). This shift was also observed with several hydrochemical parameters (Pipko et al., 2005, 2011).

The wide range of δ^{13}C signatures can be attributed to compositional differences and the degree of biogeochemical processing of the OM. It also reflects different contributions from the two dominating sources: planktogenic and terrigenous OC (e.g. Galimov, 1981; Kodina et al., 2000). The contribution of terrestrial OC was determined by using a two sources isotopic mixing model of Walsh (1989) (see Supplementary Results and discussion S3). For the terrigenous δ^{13}C values, we used the lightest isotopic composition for each year of observations: −27.6 ‰ (Dudarev et al., 2006 a, b; 2015; Semiletov et al., 2005; 2011; 2012; Naidu et al., 2000; Sanchez-Garcia et al., 2014; Vonk et al., 2014). TerrOC fractions for 2000–2008 ranged between 33 and 99 % in the surface and near bottom waters of the WBP and 1–86 % in the EBP (Table 5; Fig. 10). For the WBP and the EBP, the long-term mean values were 62 ± 9.0 % and 40 ± 13.6 %, respectively, i.e. an eastward decrease of terrOC values was oserved. In other words, the proportion of marine plankton in the POC increased from 38 % to 60 % from west to east in the ESS, which is driven by ecological changes. For example, decreasing SPM content and increasing salinity foster photosynthesis. This can be shown by a positive linear relationship between the enriched δ^{13}C isotope and salinity values (R^2 = 0.69), δ^{13}C isotope and temperature (R^2 = 0.78). A positive linear relationship was established between TN-POC (R^2 = 0.68–0.97) and δ^{15}N-δ^{13}C (R^2 = 0.86–0.87). We also see a positive linear relationship between δ^{15}N and δ^{13}C, which indicates an increase in the influence of marine plankton through increasing δ^{15}N values and increasing δ^{13}C ratios. Inverse linear relationships were observed between POC/TN-δ^{13}C (R^2 = 0.81) and SPM-δ^{13}C (R^2 = 0.65). The POC/TN values, usually taken as the signal of marine POC, reflected the influence of both isotopically light allochthonous and isotopically heavier autochthonous OM (Figs. S14-S16).

Using ^{13}C and ^{14}C isotope signals from marine, riverine and erosion sources of POC in a Monte Carlo mixing model, the relative contribution of each of the end members was estimated (Vonk et al., 2010; 2014; Karlsson et al., 2011; 2015, 2016; Sanchez-Garcia et al., 2011; 2014). This shows that the POC composition in the Dmitry Laptev Strait (station YS-23) is formed due to similarly large contributions from ICD erosion and riverine (topsoil) sources (Supplementary Figure S17 and Table S1). Already 200 km east of the Strait (station YS-26), the riverine contribution (topsoil) increases by a third. This transition is likely caused by the sedimentological properties of the material, with erosion POC (larger in size and mineral-associations) more subject to settling and riverine POC (finer particles) more prone to stay in suspension.

Calculated OC source contributions indicate exclusively terrigenous genesis (erosion + riverine) of the SPM and OC in the bottom sediments, which is also indicated by the δ^{13}C and terrOC values. At the same time, the POC/TN ratio for SPM is more consistent with the mixed and marine source, which is also supported by the terrOC values. This offset shows that both methods of source apportionment are associated with uncertainties. The POC/TN ratios are difficult to interpret due to varying contributions of the main sources and the degree of transformation during transport (Lew, 1997). In comparison with SPM, the TN content in bottom sediments decreases by more than one order of magnitude, which leads to an increase in the C/N ratios and increasing age of the OM. The latter indicator suggests that its source is the Holocene sediments, which are younger than the ICD.

The results of source apportionments show changes in the contribution of marine, riverine and erosion POC in a 513 km long transect along the Kolyma Paleovalley (Table S2; Fig. 3b, section XI). Sampling stations were located at a distance 46–513 km from the river delta and follow the Kolyma Paleovalley). The depth range was 10–43 m. The range of surface salinity values ranged from 17.8 ‰ (YS-34B) to 27.5–29.3 ‰ (YS-35 - YS-41). Station YS-34B is therefore most strongly river-influenced which is supported by the depleted δ^{13}C value of − 29.1 ‰. At the same time, the POC/TN ratios were < 5.8 along the entire transect, which are not consistent with the typical POC values for marine and terrigenous sources. Molecular biomarkers provided additional information about POC sources. The carbon preference index (CPI) of *n*-alkanes ranged from 0.9 to 2.5, CPI of *n*-alkanoic acids varied from 3.7 to 7.9. According to Rieley et al. (1991), a CPI > 5 is usually characteristic for living plants, with a tendency to decrease during OM degradation and aging. The contribution of terrestrial OM is confirmed by the high molecular weight (HMW) *n*-alkanes content (up to 517 μg/g OC) and HMW *n*-alkanoic acids content (up to 809 μg/g OC), indicating the presence of leaf waxes only produced by higher plants. A high HMW / LMW (low-molecular weight) *n*-alkane ratio also indicates the overwhelming role of terrigenous OM along the entire transect. At the same time, some values also suggest the contribution of a marine plankton source (Vetrov et al., 2008). The origin of terrestrial OM can be associated with both terrestrial vegetation and products of the eroded top

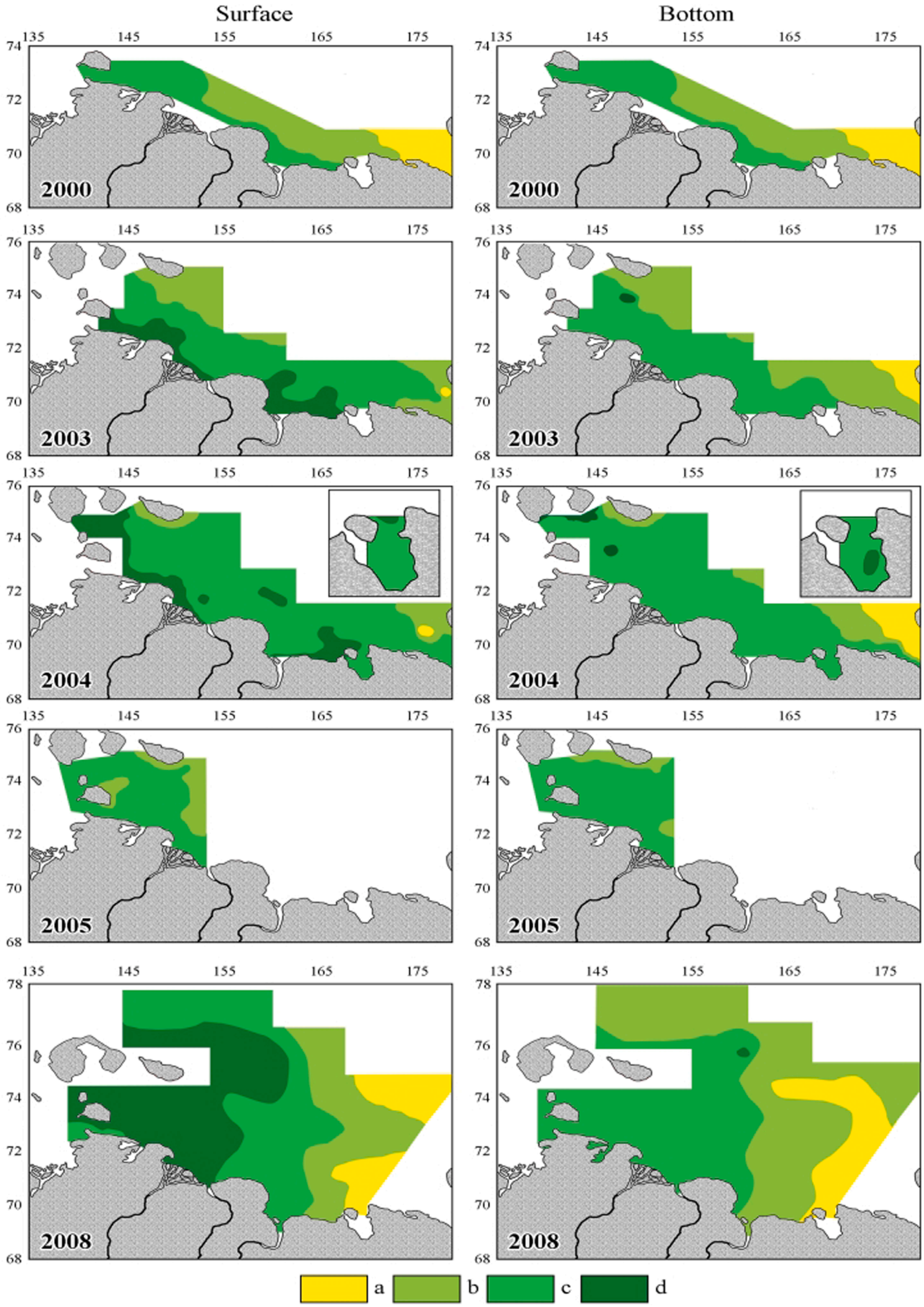

Fig. 10. TerrOC contribution to the POC pool during 2000, 2003, 2004, 2005 and 2008. TerrOC (%): a – 0–25, b – 25–50, c – 50–75, d – 75–100.

soils of the Lower Kolyma Lowland, for example, *Sphagnum* mosses. Hence, there are increased values of the C_{25} / (C_{25} + C_{29}) ratio of 0.84 close to the river outlet relative to the average of 0.66. Radiocarbon isotope signatures of the surface POC were ^{14}C = -75.0 - −27.9 ‰, which correspond to a conventional ^{14}C age of ~ 600 ÷ 200 years BP. The "youngest" POC was found only at stations in the middle of the transect (YS-37, YS-39), while "old" POC was found at the start and the end of the transect (YS-34B, YS-35, YS-41). At the start of the transect, ^{13}C-depleted carbon is associated with the lateral transport of insoluble plant detritus. This is supported by the presence of long-chain *n*-alkanes - markers of higher plant waxes – as well as high values of the CPI *n*-alkanoic acids (Vonk et al. 2010). It was shown that the age of the "young" POC of arctic and subarctic marine phytoplankton is between 85 and 500 years old and is ^{13}C-enriched (Key et al., 2004). At the same time, "older" POC plankton with ages of 1000 years and higher is characterized by a mixed isotope signal (Table S2**)**. "Young" POC has an increased HMW/LMW ratio of *n*-alkanes (1.5 times higher than the "old" one) and a CPI of 20–30*n*-alkanoic acids (1.6 times higher), but lower HMW, C_{25}/(C_{25} + C_{29}) ratio and CPI of 21–31n-alkanes (2.4, 1.4 and 1.3 times lower, respectively). The concentration of HMW *n*-alkanoic acids in "young" POC is 3.5 times lower than in "old" POC.

Thus, about 2/3 of the ESS area confined to the outer shelf was characterized by isotopically light but "old" terrigenous POC with δ^{13}C values at ~ -27 ‰. A similar situation was observed on the inner shelf of the Kara and Beaufort Seas (Kodina et al., 1999; 2008; Petrova et al., 2010; Naidu et al., 2000). Beyond the shelf edge and on the upper ice-free part of the continental slope, an intensive plankton production was observed, which resulted in the rapid increase of marine planktogenic POC. On the upper part of the continental slope, POC is characterized by "young" and isotopically heavy Arctic plankton with δ^{13}C values around –22 ‰. The influence of the marine source to the POC is also well traceable towards the coast along the Kolyma River Paleo-valley, where the source changes from marine to mixed terrigenous-marine. In the adjacent Chukchi Sea, isotopically heavy POC enters the Chukchi Peninsula through the Herald Canyon.

5. Conclusions

Our multi-year observations during the ice-free summer months provide a deeper understanding of the temporal and spatial variability as well as the transport and fate of terrigenous and marine SPM in the land-shelf system of the ESAS. The SPM distribution and its biogeochemical signature demonstrated strong spatial variability. From west to east in the ESS we observed an overall decline in the SPM content along with an increase in POC concentration, depletion of the δ^{13}C values and δ^{15}N enrichment revealing a general decrease of terrOC contribution.

In the EPB, the SPM mean concentration is approximately an order of magnitude lower than in the WBP. The contribution of terrOC in the EBP is also reduced by up to 2 times if compared to the WBP. This is reflected in the carbon and nitrogen isotopic composition: δ^{13}C signatures are heavier by 1.1 ‰ in the EBP, while ^{15}N values become 1.6 ‰ lighter than those in the WBP. TN content observed in the EBP is up to 40 % higher than in the WBP; in contrast, average C/N ratios in the EBP are lower than that in WBP by on average 0.5 units.

For the first time, this study showed constant west-to-east spatial patterns during multiple years. Contrasting elemental and isotopic characteristics of the SPM are strongly affected by relative contributions of the terrestrial vs marine OM sources and the degree of biogeochemical transformation. The "west-to-east" trend is largely determined by physical-ecological conditions during the ice-free periods that follow a decline in turbidity, increasing salinity and decreasing water temperatures from west to east. This is caused by declining volumes of both river runoff and sedimentary input (fluvial and ICD) along with a growing influence of pacific waters from west to east. The long-term average boundary between these two provinces and their SPM patterns and properties is located near 165°E. This boundary can migrate tens to hundreds of kilometers west or eastwards following changes in atmospheric circulation, and associated water circulation and ice transport regimes.

Declaration of Competing Interest

The authors declare that they have no known competing financial interests or personal relationships that could have appeared to influence the work reported in this paper.

Data availability

Data will be made available on request.

Acknowledgments

This work was supported by the Russian Science Foundation (grant 21-77-30001 to IS). Field campaigns were supported by the assignement of the Russian Ministry of Science and Higher Education (theme 0211-2021-0010 to the POI) as well as by the Knut and Alice Wallenberg Foundation (KAW contract 2011.0027 to ÖG). Furthermore, this study was partly supported by the Russian Science Foundation (grant nos. 19-17-00058 to AC, 21-17-00027 to IP). Additional support was provided by the Russian Foundation for Basic Research (grant no. 20-05-00545 to SP) and by grants from the President of the Russian Federation to support young Russian scientists (projects MK-1774.2021.1.5 to AR and MK-3476.2021.1.5 to EG). Gap filling samples from the western ESS were supported by the Russian Ministry of Science and Higher Education (grant ID: 075-15-2020-928) to the HSE. Further support was provided by the Swedish Research Council (grant 2021-06670 to JM, grant 2017-01601 to ÖG).

Appendix A. Supplementary data

Supplementary data to this article can be found online at https://doi.org/10.1016/j.pocean.2022.102903.

References

Anderson, L.G., Björk, G., Jutterström, S., Pipko, I., Shakhova, N., Semiletov, I., Wåhlström, I., 2011. East Siberian Sea, an Arctic region of very high biogeochemical activity. Biogeosciences 8, 1745–1754. https://doi.org/10.5194/bg-8-1745-2011.

Anderson, L.G., Andersson, P.S., Björk, G., Peter Jones, E., Jutterström, S., Wåhlström, I., 2013. Source and formation of the upper halocline of the Arctic Ocean. J. Geophys. Res. Oceans 118, 410–421. https://doi.org/10.1029/2012JC008291.

Anikiev, V.V., Shumilin, E.N., Dudarev, O.V., Botsul, A.I., Zakharova, P.V., Kolesov, G. M., Sapozhnikov, D.Y., Smith, R., 2004. Spatial variability in the distribution of lithological characteristics and chemical elements in the bottom sediments of the South China Sea near the Mekong and Saigon river deltas. Geochemistry International 39 (12), 1154–1171.

Biskaborn, B., Smith, S., Noetzli, J., Matthes, H., Vieira, G., Streletskiy, D., Schoeneich, P., Romanovsky, V., Lewkowicz, A., Abramov, A., Allard, M., Boike, J., Cable, W., Christiansen, H., Delaloye, R., Diekmann, B., Drozdov, D., Etzelmüller, B., Grosse, G., Lantuit, H., 2019. Permafrost is warming at a global scale. Nature Communications 10, 264. https://doi.org/10.1038/s41467-018-08240-4.

Bröder, L., Tesi, T., Tesi, T., Salvadó, J.A., Semiletov, I.P., Dudarev, O.V., Gustafsson, Ö., 2016. Fate of terrigenous organic matter across the Laptev Sea from the mouth of the Lena River to the deep sea of the Arctic interior. Biogeosciences 13 (17), 5003–5019.

Cao, P., Hu, F., Gu, G., Zhou, Y., 1986. Relationship between suspended sediments from the Changjiang estuary and the evolution of the embayed muddy coast of the Zhejiang Province. Int. Geomorphology I, 1087–1098.

Charkin, A.N., Dudarev, O.V., Semiletov, I.P., Kruhmalev, A.V., Vonk, J.E., Sánchez-García, L., Karlsson, E., Gustafsson, Ö., 2011. Seasonal and interannual variability of sedimentation and organic matter distribution in the Buor-Khaya Gulf: the primary recipient of input from Lena River and coastal erosion in the southeast Laptev Sea. Biogeosciences 8, 2581–2594. https://doi.org/10.5194/bg-8-2581-2011.

Charkin, A.N., Dudarev, O.V., Shakhova, N.E., Semiletov, I.P., Pipko, I.I., Pugach, S.P., Sergienko, V.I., 2015. Peculiarities of the Formation of Suspended Particulate Matter Fields in the Eastern Arctic Seas. Doklady Earth Sciences 462 (2), 626–630.

DeMaster, D.J., Liu, J.P., Eidam, E., Nittrouer, C.A., Nguyen, T.T., 2017. Determining rates of sediment accumulation on the Mekong shelf: Timescales, steady-state assumptions, and radiochemical tracers. Continental Shelf Research 147, 182–196.

Doğrul Selver, A., Sparkes, R.B., Bischoff, J., Talbot, H.M., Gustafsson, Ö., Semiletov, I.P., Dudarev, O.V., Boult, S., van Dongen, B.E., 2015. Distributions of bacterial and

archaeal membrane lipids in surface sediments reflect differences in input and loss of terrestrial organic carbon along a cross-shelf Arctic transect. Organic Geochemistry 83–84, 16–26.
Dudarev, O.V., Semiletov, I.P., Botsul, A.I., Charkin, A.N., 2003. Modern sedimentation in the coastal cryolithozone of the Dmitry Laptev Strait. East-Siberian Sea, Pacific Geology 22 (1), 51–60 in Russian.
Dudarev, O.V., Semiletov, I.P., Charkin, A.N., 2006a. Particulate material composition in the Lena River-Laptev Sea system: scales of heterogeneities. Doklady Earth Sciences 411A, 1445–1451.
Dudarev, O.V., Semiletov, I.P., Charkin, A.N., Botsul, A.I., 2006b. Deposition settings on the continental shelf of the East-Siberian Sea. Doklady Earth Sciences 409A (6), 1000–1005.
Dudarev, O.V., Charkin, A.N., Semiletov, I.P., Shilo, I.N., Salyuk, A.N., Spivak, E.A., 2008. The current state of submarine island relicts on the East Siberian shelf. Doklady Earth Sciences 419 (1), 352–358.
Dudarev, O.V., Charkin, A.N., Shakhova, N.E., Sergienko, V.I., Pipko, I.I., Pugach, S.P., Chernykh, D.V., 2015. Peculiarities of the present-day morpholithogenesis on the Laptev Sea Shelf: Semenovskaya shoal (Vasema Land). Dokl. Earth Sci. 462, 510–516. https://doi.org/10.1134/S1028334X15050116.
Dudarev, O.V.: Litomorphogenesis on the East Arctic, thesis of doctor dissertation, Vladivostok, 48 pp., 2016 (in Russian).
Feng, X., Vonk, J.E., van Dongen, B.E., Gustafsson, O., Semiletov, I.P., Dudarev, O.V., Wang, Z., Montucon, D.B., Wacker, L., Eglinton, T.I., 2013. Differential mobilization of terrestrial carbon pools in Eurasian Arctic river basins. P. Natl. Acad. Sci. USA 110, 14168–14173. https://doi.org/10.1073/pnas.1307031110.
Feng, X., Gustafsson, Ö., Holmes, R.M., Vonk, J.E., van Dongen, B.E., Semiletov, I.P., Dudarev, O.V., Yunker, M.B., Macdonald, R.W., Montluçon, D.B., Eglinton, T.I., 2015a. Multi-molecular tracers of terrestrial carbon transfer across the pan-Arctic: comparison of hydrolyzable components with plant wax lipids and lignin phenols. Biogeosciences 12, 4841–4860. https://doi.org/10.5194/bg-12-4841-2015.
Feng, X., Gustafsson, Ö., Holmes, R.M., Vonk, J.E., van Dongen, B.E., Semiletov, I.P., Dudarev, O.V., Yunker, M.B., Macdonald, R.W., Wacker, L., Montluçon, D.B., Eglinton, T.I., 2015b. Multi-molecular tracers of terrestrial carbon transfer across the pan-Arctic: 14C characteristics of sedimentary carbon components and their environmental controls. Global Biogeochem. Cycles 29, 1855–1873. https://doi.org/10.1002/2015GB005204.
Galimov, E.M., 1981. The nature of biological fractioning of isotopes. Nauka, Moscow. 247 pp., (in Russian).
Geoecology of shelf and coasts of Russian Seas, edited by N.A. Aibulatov, Moscow: Neosphera, 428 pp., 2001 (in Russian).
Gordeev, V.V., Martin, J.M., Sidorov, I.S., Sidorova, M.V., 1996. A reassessment of the Eurasian river input of water, sediment, major elements, and nutrients to the Arctic Ocean. Amer. J. Sci. 296, 664–691.
Gordeev, V.V., Rachold, V., 2004. River input. In: Organic Carbon Cycle in the Arctic Ocean: Present and Past. Springer Verlag, Berlin, Germany, pp. 39–46.
Grigoryev, N.F., Rachold, V., Hubberten, H.-W., Schirrmeister, L., 2004. Organic carbon input to the Arctic Seas through coastal erosion. In: Stein, R., Macdonald, R.W. (Eds.), Organic Carbon Cycle in the Arctic Ocean: Present and Past. Springer Verlag, Berlin, Germany, pp. 41–47.
Guo, L., Santschi, P.H., 1996. A critical evaluation of the cross-flow ultrafiltration technique for sampling of colloidal organic carbon in seawater. Mar. Chem. 55, 113–127.
Guo, L., Semiletov, I., Gustafsson, O., Ingri, J., Andersson, P., Dudarev, O., White, D., 2004. Characterization of Siberian Arctic coastal sediments: implications for terrestrial organic carbon export. Global Biogeochemical Cycles 18.
Gustafsson, O., Bucheli, T.D., Kukulska, Z., Andersson, M., Largeau, C., Rouzaud, J.N., Reddy, C.M., Eglinton, T.I., 2001. Evaluation of a protocol for the quantification of black carbon in sediments Global Biogeochem. Cycles 15, 881–890.
Gustafsson, Ö., Haghseta, F., Chan, C., MacFarlane, J., Gschwend, P.M., 1997. Quantification of the dilute sedimentary "soot-phase": Implications for PAH speciation and bioavailability. Environ. Sci. Technol. 31, 203–209.
Gustafsson, Ö., van Dongen, B.E., Vonk, J.E., Dudarev, O.V., Semiletov, I.P., 2011. Widespread release of old carbon across the Siberian Arctic echoed by its large rivers. Biogeosciences 8, 1737–1743. https://doi.org/10.5194/bg-8-1737-2011.
Hugelius, G., Strauss, J., Zubrzycki, S., Harden, J.W., Schuur, E.A.G., Ping, C.-L., Schirrmeister, L., Grosse, G., Michaelson, G.J., Koven, C.D., O'Donnell, J.A., Elberling, B., Mishra, U., Camill, P., Yu, Z., Palmtag, J., Kuhry, P., 2014. Estimated stocks of circumpolar permafrost carbon with quantified uncertainty ranges and identified data gaps. Biogeosciences 11, 6573–6593. https://doi.org/10.5194/bg-11-6573-2014.
Ivanov, V.V., Alekseev, V.A., Alekseeva, T.A., Koldunov, N.V., Repina, I.A., Smirnov, A. V., 2013. Is Arctic ice cover becoming seasonal? Issled. Zemli Kosmosa 4, 50–65 in Russian.
Karlsson, E.S., Bruchert, V., Tesi, T., Charkin, A., Dudarev, O., Semiletov, I., Gustafsson, O., 2015. Contrasting regimes for organic matter degradation in the East Siberian Sea and the Laptev Sea assessed through microbial incubations and molecular markers. Marine Chemistry 170, 11–22.
Karlsson, E.S., Charkin, A., Dudarev, O., Semiletov I., Vonk1, J. E., Sánchez-García, L., Andersson, A., Gustafsson Ö., 2011. Carbon isotopes and lipid biomarker investigation of sources, transport and degradation of terrestrial organic matter in the Buor-Khaya Bay, SE Laptev Sea. Biogeosciences 8, 1865–1879. https://doi.org/10.5194/bg-8-1865-2011.
Karlsson, E., Gelting, J., Tesi, T., van Dongen, B., Andersson, A., Semiletov, I., Charkin, A., Dudarev, O., Gustafsson, Ö., 2016. Different sources and degradation status of dissolved, particulate and sedimentary organic matter along the Eurasian Arctic coastal margin. Global Biogeochemical Cycle 30, 898–919. https://10.1002/2015GB005307.
Key, R.M., Kozyr, A., Sabine, C.L., Lee, K., Wanninkhof, R., Bullister, J.L., Feely, R.A., Millero, F.J., Mordy, C., Peng, T.-H., 2004. A global ocean carbon climatology: Results from Global Data Analysis Project (GLODAP). Global Biogeochem. Cycles 18, GB4031. https://10.1029/2004GB002247.
Kodina, L.A., Bogacheva, M.P., Vlasova, L.N., Galimov, E.M., 1999. Organic Matter of Aqueous Particulate Matter in the Yenisei Estuary: Isotope Composition, Consistent Patterns of Distribution, and Genesis. Geokhimiya 11, 1206–1217.
Kodina, L.A., Lyutsarev, S., Bogacheva, M., 2000. Sources of sedimentation material of the drift Ice of the Arctic Basin, based on the information from isotope analysis of the organic carbon of ice suspended particles. Doklady Earth Sciences 341 (4), 511–515 in Russian.
Kodina, L.A., Tokarev, V.G., Korobeynik, G.S., Vlasova, L.N., Bogacheva, M.P., 2008. Natural background of hydrocarbon gases (C1–C5) of the Kara Sea water mass. Geochemistry 7, 721–733 in Russian.
Kodina, L.A., Stepanets, O., Galimov, E., 2009. The isotope geochemistry of the organic matter and the problem concerned with radioactivity of the Kara Sea. In: the Laptev Sea System and Adjacent Seas of the Arctic. Present-day Conditions and the History of Development. Moscow State University, Moscow, pp. 122–136 in Russian.
Kulakov, M.Y., 2008. Water circulation and transport of suspended sediments in the Laptev and East-Siberian Seas. Problems of Arctic and Antarctic 3 (80), 89–97 in Russian.
Lew, M., 1997. The distribution of some major and trace elements in sediments of the Atlantic Ocean: The distribution of total, fixed and organic nitrogen. Chem. Geol. 33, 225–235.
Martens, J., Wild, B., Muschitiello, F., O'Regan, M., Jakobsson, M., Semiletov, I.P., Dudarev, O.V., Gustafsson, Ö., 2020. Remobilization of dormant carbon from Siberian-Arctic permafrost during three past warming events. Sci. Adv. 6 (42), eabb6546.
Martens, J., Romankevich, E., Semiletov, I., Wild, B., van Dongen, B., Vonk, J., Tesi, T., Shakhova, N., Dudarev, O.V., Kosmach, D., Vetrov, A., Lobkovsky, L., Belyaev, N., Macdonald, R.W., Pieńkowski, A.J., Eglinton, T.I., Haghipour, N., Dahle, S., Carroll, M.L., Åström, E.K.L., Grebmeier, J.M., Cooper, L.W., Possnert, G., Gustafsson, Ö., 2021. CASCADE – The Circum-Arctic Sediment CArbon DatabasE. Earth Syst. Sci. Data 13, 2561–2572. https://doi.org/10.5194/essd-13-2561-2021.
McClelland, J.W., Holmes, R.M., Peterson, B.J., Raymond, P.A., Striegl, R.G., Zhulidov, A.V., Zimov, S.A., Zimov, N., Tank, S.E., Spencer, R.G.M., Staples, R., Gurtovaya, T.Y., Griffin, C.G., 2016. Particulate organic carbon and nitrogen export from major Arctic rivers. Global Biogeochem. Cycles 30, 629–643.
Minsley, B.J., Abraham, J.D., Smith, B.D., Cannia, J.C., Voss, C.I., Jorgenson, M.T., Walvoord, M.A., Wylie, B.K., Anderson, L., Ball, L.B., Deszcz-Pan, M., Wellman, T.P., Ager, T.A., 2012. Airborne electromagnetic imaging of discontinuous permafrost. Geophys. Res. Lett. 39, L02503. https://doi.org/10.1029/2011GL050079.
Naidu, A., Cooper, L., Finney, B., Macdonald, R.W., Alexander, C., Semiletov, I.P., 2000. Organic carbon isotope ratios ($\delta^{13}C$) of Arctic Amerasian Continental shelf sediment. Int. J Earth Sci. 89 (522) https://doi.org/10.1007/s005310000121.
Navigation Book of the East-Siberian Sea, 1998. Publication of GUNIO MO Russian Federation, St. Petersburg, 207 pp., (in Russian).
Nikiforov, Ye.G., Shpaikher, A.O., 1980. Features of the formation of Hydrological Regime Large-scale variations in the Arctic ocean. Hydrometeoizdat, Leningrad, 269 p., (in Russian).
Osadchiev, A., Frey, D., Spivak, E., Shchuka, S., Tilinina, N., Semiletov, I., 2021. Structure and Inter-Annual Variability of the Freshened Surface Layer in the Laptev and East-Siberian Seas During Ice-Free Periods. Frontiers in Marine Science 8, 735011. https://doi.org/10.3389/fmars.2021.735011.
Petrova, V.I., Batova, G.I., Kursheva, A.V., Litvinenko, L.V., Konovalov, D.A., 2010. Organic matter in the bottom sediments of the Ob Bay: distribution, nature, and sources. Geochemistry Intern. 48 (2), 140–151.
Pipko, I.I., Semiletov, I.P., Pugach, S.P., 2005. The carbonate system of the East Siberian Sea waters. Doklady Earth Sciences 402 (4), 624–627.
Pipko, I.I., Semiletov, I.P., Pugach, S.P., Wáhlström, I., Anderson, L.G., 2011. Interannual variability of air-sea CO2 fluxes and carbon system in the East Siberian Sea. Biogeosciences 8, 1987–2007. https://doi.org/10.5194/bg-8-1987-2011.
Proshutinsky, A.Y., Johnson, M.A., 1997. Two circulation regimes of the wind-driven Arctic Ocean. J. Geophys. Res. 102 (C6), 12493–12514.
Proshutinsky, A., Timmermans, M.-L., Ashik, I., Beszczynska-Moeller, A., Carmack, E., Frolov, I., Ingvaldsen, R., Itoh, M., Kikuchi, T., Krishfield, R., McLaughlin, F., Loeng, H., Nishino, S., Puickart, R., Rabe, B., Rudels, B., Semiletov, I., Schauer, U., Shakhova, N., Shimada, K., Sokolov, V., Steele, M., Toole, J., Weingarther, T., Williams, W., Woodgate, R., Yamamoto-Kawai, M., Zimmermann, S., 2012. The Arctic] Ocean [in "State of the Climate in 2011". Bulletin of the American Meteorological Society 93 (7), S142–S145.
Pugach, S.P., Pipko, I.I., 2013. Dynamics of Colored Dissolved Matter on the East Siberian Sea Shelf. Doklady Earth Sciences 448 (1), 153–156.
Pugach, S.P., Pipko, I.I., Semiletov, I.P., Sergienko, V.I., 2015. Optical Characteristics of the Colored Dissolved Organic Matter on the East Siberian Shelf. Doklady Earth Sciences 465 (2), 1293–1296.
Pugach, S.P., Pipko, I.I., Shakhova, N.E., Shirshin, E.A., Perminova, I.V., Gustafsson, O., Bondur, V.G., Ruban, A.S., Semiletov, I.P., 2018. Dissolved organic matter and its optical characteristics in the Laptev and East Siberian seas: spatial distribution and interannual variability (2003–2011). Ocean Sci. 14, 87–103. https://doi.org/10.5194/os-14-87-2018.
Rachold, V., Are, F.E., Atkinson, D.E., Cherkashov, G., Solomon, S.M., 2003. Arctic Coastal Dynamics (ACD): an introduction. Geo-Mar. Lett. 25, 63–68. https://doi.org/10.1007/s00367-004-0187-9.

Rieley, G., Collier, R.J., Jones, D.M., Eglinton, G., 1991. Biogeochemistry of Ellesmere Lake, U.K. I. Source correlation of leaf wax inputs to the sedimentary lipid record. Org. Geochem. 17, 901–912.

Salvadó, J.A., Tesi, T., Andersson, A., Ingri, J., Dudarev, O.V., Semiletov, I.P., Gustafsson, Ö., 2015. Organic carbon remobilized from thawing permafrost is resequestered by reactive iron on the Eurasian Arctic Shelf. Geophys. Res. Letters 42. https://doi.org/10.1002/2015GL066058.

Salvadó, J.A., Tesi, T., Sundbom, M., Karlsson, E., Krusa, M., Semiletov, I.P., Panova, E., Gustafsson, Ö., 2016. Contrasting composition of terrigenous orcanic matter in the dissolved, particulate and sedimentary organic carbon pools on the outer East Siberian Arctic Shelf. Biogeosciences 13 (22), 6121–6138.

Sánchez-García, L., Alling, V., Pugach, S., Vonk, J., van Dongen, B., Humborg, C., Dudarev, O., Semiletov, I., Gustafsson, Ö., 2011. Inventories and behavior of particulate organic carbon in the Laptev and East Siberian seas. Global Biogeochem. Cy. 25, GB2007. https://doi.org/10.1029/2010GB003862.

Sánchez-García, L., Vonk, J.E., Charkin, A.N., Kosmach, D., Dudarev, O.V., Semiletov, I. P., Gustafsson, Ö., 2014. Characterisation of Three Regimes of Collapsing Arctic Ice Complex Deposits on the SE Laptev Sea Coast using Biomarkers and Dual Carbon Isotopes. Permafrost and Periglac. Process 25, 172–183.

Savelieva, N.I., Semiletov, I.P., Vasilevskaya, L.N., Pugach, S.P., 2000. A climate shift in seasonal values of meteorological and hydrological parameters for Northeastern Asia. Progress in Oceanography 47 (2–4), 279–297.

Savelyeva, N.I., Semiletov, I.P., Pipko, I.I., 2008. Influence of meteorological processes and river runoff on the thermohaline structure of the littoral zone water of the East Siberian Sea. Meteorology and hydrology 4, 63–72 in Russian.

Schuur, E., McGuire, A., Schädel, C., Grosse, G., Harden, J.W., Hayes, D.J., Hugelius, G., Koven, C.D., Kuhry, P., Lawrence, D.M., Natali, M.N., Olefeldt, D., Romanovsky, V. E., Schaefer, K., Turetsky, M.R., Treat, C.C., Vonk, J.E., 2015. Climate change and the permafrost carbon feedback. Nature 520, 171–179. https://doi.org/10.1038/nature14338.

Semiletov, I.P., 1999. On aquatic sources and sinks of CO_2 and CH_4 in the Polar Regions. J. Atmos. Sci. 56, 286–306.

Semiletov, I., Dudarev, O., Luchin, V., Charkin, A., Shin, K.-H., Tanaka, N., 2005. The East Siberian Sea as a transition zone between Pacific-derived waters and Arctic shelf waters. Geophys. Res. Lett. 32, L10614. https://doi.org/10.1029/2005GL022490.

Semiletov, I.P., Pipko, I.I., Shakhova, N.E., Dudarev, O.V., Pugach, S.P., Charkin, A.N., McRoy, C.P., Kosmach, D.A., Gustafsson, O., 2011. Carbon transport by the Lena River from its headwaters to the Arctic Ocean, with emphasis on fluvial input of terrestrial particulate organic carbon vs. carbon transport by coastal erosion. Biogeosciences 8, 1–20.

Semiletov, I., Pipko, I., Gustafsson, Ö., Anderson, L.G., Sergienko, V., Pugach, S., Dudarev, O., Charkin, A., Gukov, A., Bröder, L., Andersson, A., Spivak, E., Shakhova, N., 2016. Acidification of East Siberian Arctic Shelf waters through addition of freshwater and terrestrial carbon. Nature Geoscience 9, 361–365. https://doi.org/10.1038/ngeo2695.

Semiletov, I.P., Savelieva, N.I., Weller, G.E., Pipko, I.I., Pugach, S.P., Gukov, A.Y., Vasilevskaya, L.N., 2000. The dispersion of Siberian river flows into coastal waters: Meteorological, hydrological and hydrochemical aspects. In: Lewis, E.L. (Ed.), the Freshwater Budget of the Arctic Ocean. Kluwer Academic Publishers, Dordrecht, Meeting/NATO ASI Series, pp. 323–366.

Semiletov, I.P., Shakhova, N.E., Sergienko, V.I., Pipko, I.I., Dudarev, O., 2012. On Carbon Transport and Fate in the East Siberian Arctic Land-Shelf-Atmosphere System. Environment Research Letters 7. https://doi.org/10.1088/1748-9326/7/1/015201.

Shevchenko, V.P., Lisitzin, A.P., 2004. Aeolan Input // The organic carbon cycle in the Arctic Ocean. Eds. R. Stein, R.W. Macdonald. Berlin: Springer Verlag, 2004. P. 53-54.

Stein, R., Macdonald, R.W. (Eds.), 2004. the Organic Carbon Cycle in the Arctic Ocean. Berlin, Springer, p. 363.

Stein, R., Nurnberg, D., 1995. Reports on Polar Research. Bremerhaven: AWI 176, 286–296.

Sternberg, R., Larsen, L., Miao, Y., 1985. Tidally driven sediment transport on the East China Sea continental shelf. Cont. Shelf Res. 4 (1–2), 105–120.

Tesi, T., Semiletov, I., Hugelius, G., Dudarev, O., Kuhry, P., Gustafsson, O., 2014. Composition and fate of terrigenous organic matter along the Arctic land-ocean continuum in East Siberia: Insights from biomarkers and carbon isotopes. Geochimica et Cosmochimica Acta 133, 235–256.

Tesi, T., Semiletov, I., Dudarev, O., Andersson, A., Gustafsson, Ö., 2016. Matrix association effects onhydrodynamic sorting and degradation of terrestrial organic matter during cross-shelf transport in the Laptev and East Siberian shelf seas. J. Geophys. Res. Biogeosci. 121 https://doi.org/10.1002/2015JG003067.

Turetsky, M.R., Abbott, B.W., Jones, M.C., Anthony, K.W., Olefeldt, D., Schuur, E.A.G., Grosse, G., Kuhry, P., Hugelius, G., Koven, C., Lawrence, D.M., Gibson, C., Sannel, A. Britta K., McGuire, A.D., 2020. Carbon release through abrupt permafrost thaw. Nature Geoscience 13 (8) https://doi.org/10.1038/s41561-019-0526-0.

van Dongen, B.E., Semiletov, I.P., Weijers, J.W.H., Gustafsson, Ö., 2008. Contrasting lipid biomarker composition of terrestrial organic matter exported from across the Eurasian Arctic by the five Great Russian Arctic Rivers. Global Biogeochemical Cycles 22, GB1011. https://doi.org/10.1029/2007GB002974.

Vetrov, A.A., Romankevich, E.A., 2004. Carbon cycle in the Russian Arctic Seas. Springer – Verlag, Berlin, p. 331 pp..

Vetrov, A.A., Romankevich, E.A., 2011. Genesis of organic matter in the Kara Sea bottom sediments. Oceanology 51 (4), 608–615. https://doi.org/10.1134/S0001437011040187.

Vetrov, A.A., Semiletov, I.P., Dudarev, O., Peresypkin, V.I., Charkin, A.N., 2008. Composition and genesis of the organic matter in the bottom sediments on the East Siberian Sea. Geochem. Int. 46, 156–167.

Vinogradov, G.M., Druzhkov, N.V., Marasaeva, E.F., Larionov, V.V., 2001. The under-ice mesozooplankton of the Pechora and Kara seas in the winter-spring period, 2000. Oceanology (Engl. Transl.) 41 (5), 696–702.

Vonk, J.E., Gustafsson, Ö., 2013. Permafrost-carbon complexities. Nature Geoscience 6 (9), 675–676.

Vonk, J.E., Sánchez-García, L., Semiletov, I., Dudarev, O., Eglinton, T., Andersson, A., Gustafsson, Ö., 2010. Molecular and radiocarbon constraints on sources and degradation of terrestrial organic carbon along the Kolyma paleoriver transect, East Siberian Sea. Biogeosciences 7, 3153–3166. https://doi.org/10.5194/bg-7-3153-2010.

Vonk, J.E., Sánchez-García, L., van Dongen, B.E., Alling, V., Kosmach, D., Charkin, A., Semiletov, I.P., Dudarev, O.V., Shakhova, N., Roos, P., Eglinton, T.I., Andersson, A., Gustafsson, Ö., 2012. Activation of old carbon by erosion of coastal and subsea permafrost in Arctic Siberia. Nature 489, 137–140.

Vonk, J.E., Semiletov, I.P., Dudarev, O.V., Eglington, T.I., Andersson, A., Shakhova, N., Charkin, A., Heim, B., Gustafsson, O., 2014. Preferential burial of permafrost-derived organic carbon in Siberian – Arctic shelf waters. J. Geophysical Research 119. https://doi.org/10.1002/2014JC010261.

Walsh, J.J., McRoy, C.P., Coachman, L.K., Goering, J.J., Nihoul, J.J., Whitledge, T.E., Blackburn, T.H., Parker, P.L., Wirick, C.D., Shuert, P.G., Grebmeier, J.M., Springer, A.M., Tripp, R.D., Hansell, D.A., Djenidi, S., Deleersnijder, E., Henriksen, K., Lund, B. A., Andersen, P., Müller-Karger, F.E., Dean, K., 1989. Carbon and nitrogen cycling within the Bering/Chukchi Seas: source regions for organic matter effecting AOU demands of the Arctic Ocean. Prog. Oceanog 22, 277-359.

Wild, B., Andersson, A., Bröder, L., Vonk, J., Hugelius, G., McClelland W., J., Song, W., Raymond A., P., Gustafsson, Ö., 2019. Rivers across the Siberian Arctic unearth the patterns of carbon release from thawing permafrost. P. Natl. Acad. Sci. USA 116 (21), 10280–10285. https://doi.org/10.1073/pnas.1811797116.

Zhang, J., Huang, W., 1990. Effect of particle size on transition metal concentrations in the Changjiang and Huanghe, China. The Science of the Total Environment 9, 48–68.